



# Indonesian rainfall variability during Western North Pacific and Australian monsoon phase related to convectively coupled equatorial waves

Ida Pramuwardani<sup>1,2</sup> · Hartono<sup>1</sup> · Sunarto<sup>1</sup> · Ardhasena Sopaheluwakan<sup>2</sup>

Received: 11 April 2018 / Accepted: 15 October 2018 / Published online: 7 November 2018  
© Saudi Society for Geosciences 2018

## Abstract

The Indonesian archipelago which has over 15,000 islands, lies in the tropics between Asia and Australia. This eventually alters the rainfall variability over the region, which was influenced by the Asian-Australian monsoon and controlled by intraseasonal variabilities such as convectively coupled equatorial waves (CCEW), i.e., Kelvin,  $n = 1$  equatorial Rossby (ER), mixed Rossby gravity (MRG), and  $n = 1$  Westward inertio gravity (WIG), including the Madden–Julian Oscillation (MJO). This study examines a 15-year 3B42 data for trapping CCEW and MJO in the region of Indonesia during both active and extreme Western North Pacific (WNP) and Australian (AU) monsoon phases, which are then compared with 30-year rainfall anomalies among 38 synoptic stations over Indonesia. The space–time spectral analysis is employed to filter each wave including the MJO in the equator, then proceeding with the empirical orthogonal function (EOF) method to seek each wave peak which then coincides with WNP and AU monsoon peaks over Indonesia. It is concluded that an extreme monsoon classification has proven to control rainfall activity related to the CCEW and MJO at 60.66% during December through February (DJF)-WNP for only the significant wave perturbation value. Meanwhile, the CCEW and MJO significantly increase/decrease precipitation at Day 0 for about 37.88% from the total of Day 1st to Day end. Although the contribution of the CCEW and MJO does not profoundly influence rainfall activity during monsoon phase over Indonesia, they still modulate weather condition for more than 50%. On the other hand, a complex topography with a number of land–sea complexities is capable of influencing the rainfall variability in the region as a negative relationship is associated with the CCEW and MJO either during DJF-WNP or July through August (JAS)-AU monsoon phase.

**Keywords** CCEW · MJO · Rainfall variability · Indonesia · Monsoon

## Introduction

The previous study has revealed that the propagation of long-band westerly wind (10,000 km) that lasted for a period of 5 days in the upper troposphere oscillated regularly over the

tropical region (Yanai and Maruyama 1966). Despite the absence of conclusion on the existence of this wave, many studies have later focused on the tropical meteorological dynamics, especially on the disturbance system associated with wind perturbation (Yanai and Maruyama 1966; Yanai et al. 1968; Liebmann and Hendon 1990) and convection (Takayabu and Nitta 1993).

Since the tropical convection in the mid-atmosphere releases latent heat that plays a significant role in stimulating equatorial waves (Holton 2004), identifying the convectively coupled equatorial waves (CCEW) using a broad spectrum of convective/precipitating clouds becomes necessary. Lubis and Jacobi (2014) utilized remote sensing data, namely tropical rainfall-measuring mission (TRMM) 3B42 and examined the equatorial waves that coupled with convection in the formation of tropical precipitation. They also defined that the active Asia-Australia monsoon in the Maritime Continent that

---

**Electronic supplementary material** The online version of this article (<https://doi.org/10.1007/s12517-018-4003-7>) contains supplementary material, which is available to authorized users.

---

✉ Ida Pramuwardani  
ida.pramuwardani@mail.ugm.ac.id; idapramuwardani@gmail.com

<sup>1</sup> Faculty of Geography, Gadjah Mada University, Yogyakarta, Indonesia

<sup>2</sup> Meteorological Climatological and Geophysical Agency, Jakarta, Indonesia

triggered the precipitation to intensify particularly due to equatorial waves, which includes TD-type wave in this region. Meanwhile, Cho et al. (2004) distinguished the signal data using the space–time spectral analysis method that was introduced by Wheeler and Kiladis (1999) (hereafter referred to as WK99) into boreal summer and winter.

The background theory for equatorial waves was introduced by Matsuno (1966) in a famous equation named “shallow water,” which assumed that the waves oscillated transversally and were trapped in the tropical area. He then associated his equation with the dispersion relationship for both eastward and westward propagating inertio gravity (IG), equatorial Rossby (ER), Kelvin, and latter is mixed Rossby gravity (MRG). Further studies on the dispersion relationship for equatorial wave coupled with convective clouds were developed by Wheeler and Kiladis (1999). They also introduced a space–time spectral analysis method in the wavenumber ( $k$ ) and frequency ( $\omega$ ) domain (WK99) using a Fourier transform to convert space–time data series into a wavenumber–frequency domain to attain each wave type based on the meridional mode number ( $n$ ). Previous studies revealed that Kelvin waves have substantial influences over Indonesia (Kiladis et al. 2009), likewise MJO (Cho et al. 2004). This is also relevant to a previous study suggesting that the Indonesian archipelago is affected robustly by the MJO through its ability to suppress mean sea-level pressure for conducting convection over the region (Madden and Julian 1972). Meanwhile, by connecting intraseasonal variability within Indonesia, a dominant local factor from land–sea atmospheric interaction still becomes a prominent factor that controls the weather (Hidayat and Kizu 2010). Another suggestion revealed that convection over the warm pool region including Indonesia is driven by the frequency and duration of weak unorganized signals (Huang and Huang 2011), which may include its local factor. Moreover, the most recent study remarked an interaction between MJO and CCEW, even though there is a complex interaction among these phenomena over the Maritime Continent of Indonesia due to the complex terrain of the region (Kikuchi et al. 2018).

The Asian–Australian monsoon plays a significant role over Indonesia with its ability to cut down westward zonal wind and to induce westerly wave propagation (Liebmann and Hendon 1990; Wheeler and McBride 2005). Thus, monsoon plays an important aspect in coupling convection with equatorial waves. There are eight regional monsoon domains according to seasonal contrast in precipitation variability (Wang et al. 2012), two of them are the Western North Pacific (WNP) and Australian (AU) monsoon regions which then used in this study. There are two reasons why these two monsoon regions are considered; first is due to the pattern similarity between climatological annual cycles of precipitation rates of both monsoon regions (Yim et al. 2013), as well as with Indonesian rainfall annual cycle from climate region A

(Aldrian and Susanto 2003). The second reason is that WNP and AU are the monsoon domains that are closest to Indonesia (see Fig. 1). Figure 1 confirms that positive AU monsoon index reflects a rainy season in most parts of the Indonesian region, while the positive WNP monsoon index indicates otherwise, which will also be elaborated further in the “Results.” The calculation of the WNP and AU monsoon indices will describe later in the “Data and methods” section.

The objective of this study is to identify the distribution of rainfall variability based on the evolution of each type of CCEW (Kelvin, ER, MRG, and WIG) including the MJO, using remote sensing data (TRMM 3B42) in the regions of Indonesia during the WNP and AU monsoon phases. In this study, a peak of Asian monsoon is represented by the WNP monsoon index (Wang and Fan 1999; Wang et al. 2012; Yim et al. 2013), whereas the Australian monsoon is represented by the AU monsoon index (Yim et al. 2013).

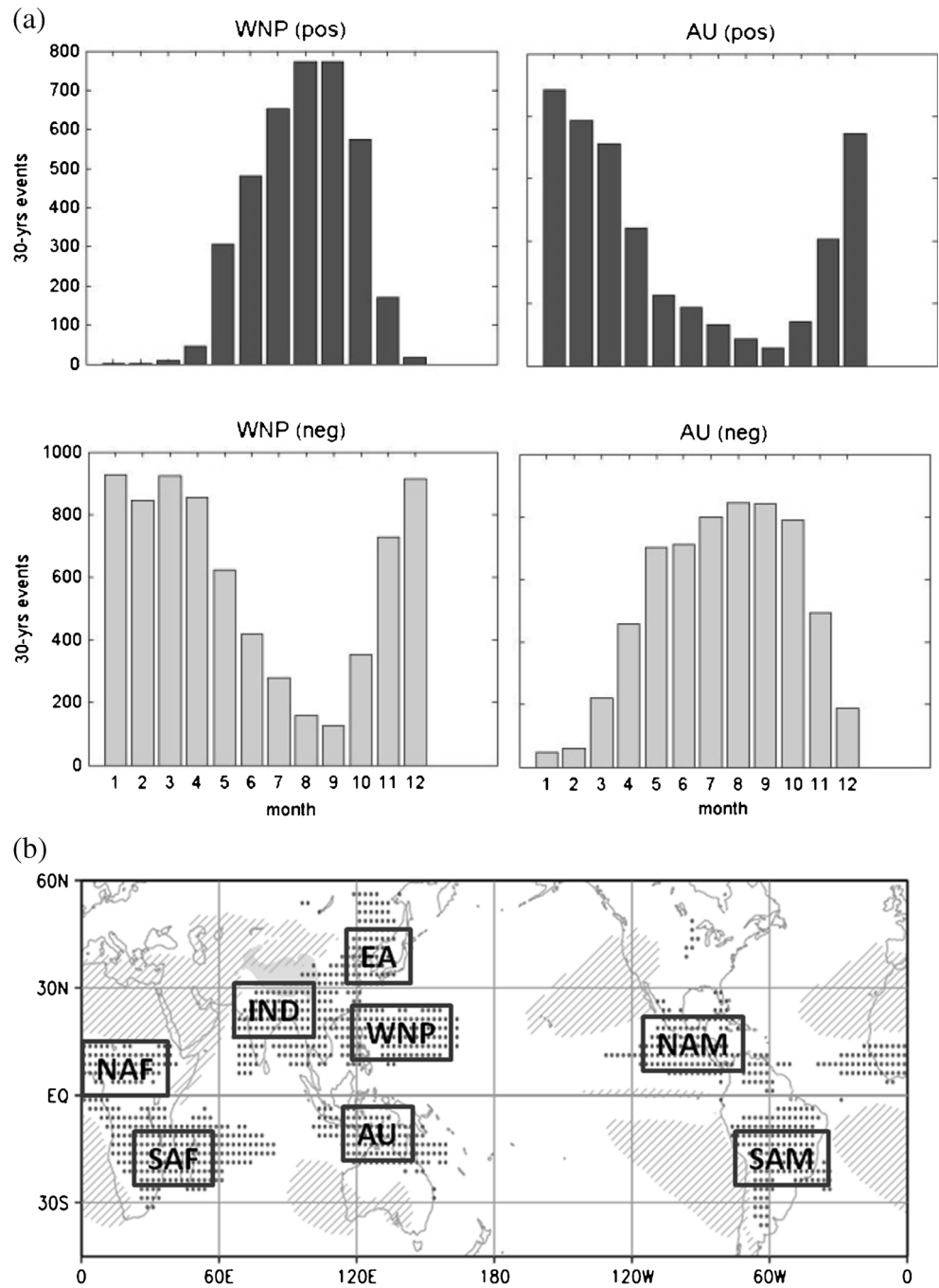
This paper is further divided into four sections. The first section describes the historical background, which mainly contains the background theories of equatorial waves and the regional monsoon that is affecting the Indonesian rainfall variability. The second section explains the data and method used to achieve the research objectives. The third section elaborates the preliminary results, including the comparison with previous studies on rainfall variability distribution related to regional monsoon indices that predominantly affect Indonesia. The last section sums up remarks and findings from the previous three sections, including confirmations with reference to previous studies and recommendation for further studies.

## Data and methods

### Data

A 15-year-long series of daily TRMM data (3B42 V7 derived) was used to estimate the tropical rainfall from 1 January 2001 to 31 December 2015. TRMM is used because of several benefits, such as continuous data acquisition, finer resolution ( $0.25 \times 0.25^\circ$ ), comprehensively merged infrared–microwave multi-satellite, and the collection and conversion of all available data into precipitation estimates (Huffman 2006). For a detailed documentation on the dataset, this research referred to the TRMM user handbook by the National Space Development Agency of Japan (NASDA 2001). A 30-year daily rainfall observation data from 1 January 1986 to 31 December 2015 of 38 synoptic stations from the Indonesian Meteorology Climatology and Geophysics Agency (BMKG) was also gathered to obtain an actual rainfall anomaly climatologically, which will later seek the relationship with each wave during each monsoon phase.

**Fig. 1** **a** Annual cycle of WNP monsoon indices for positive (upper left) and negative (bottom left), as well as for AU monsoon indices for positive (upper right) and negative (bottom right), calculated from 850 hPa zonal wind ERA-interim 30-year time series data; **b** regional precipitation domain indicated by abbreviation for each domain (figure adopted from Wang et al. 2012)

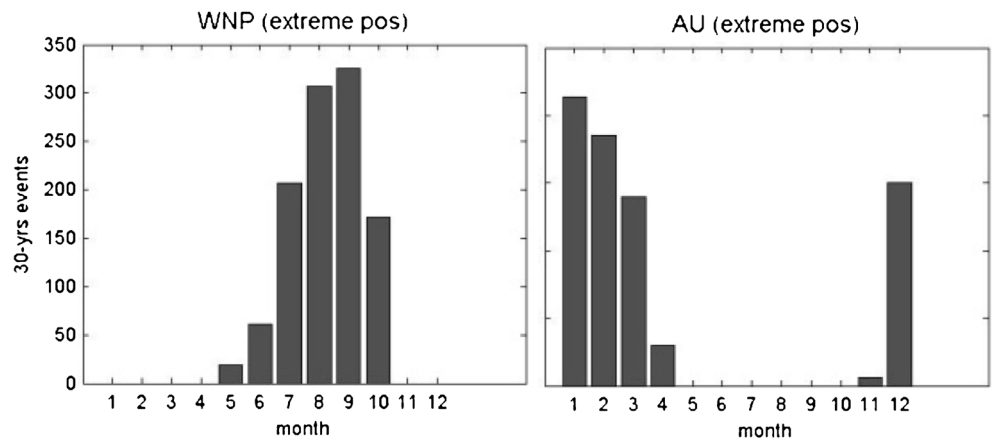


In addition, the 850-hPa zonal wind of a 30-year reanalysis data from the ERA-Interim reanalysis data from 1 January 1986 to 31 December 2015 was utilized to calculate WNP and AU indices related to Asian-Australian monsoon activity. Furthermore, a 15-year time series data from the ERA-Interim 850-hPa resultant wind which was calculated from zonal and meridional wind at the same level is also shown to complement the evolution stage of each wave to fit the 15-year 3B42 data. The ERA-Interim reanalysis data was chosen due

to its long and continuous data archive and finer spatial and temporal resolution. Moreover, it has already been assimilated many times with observation data to reduce the discrepancies with the real condition in the atmosphere (Dee 2011). In order to obtain a detailed information for the ERA-Interim reanalysis with data assimilation system, this research is referred to the same paper.

Inverse distance weight (IDW) method was applied to reduce any delays and costs of running the

**Fig. 2** An annual cycle of extreme positive indices for WNP monsoon (left) and AU monsoon (right)



mathematical codes for a very long dataset in the computer. On the other hand, heterogeneous spatial data was also analyzed by grid for both the 3B42 and ERA-Interim datasets.

**Methods**

First of all, monsoon indices were calculated to define the regional monsoon phase peak activity, which was then

**Fig. 3** Seasonal mean rainfall during DJF-WNP monsoon (upper) and during JAS-AU monsoon (below) from 38 synoptic stations

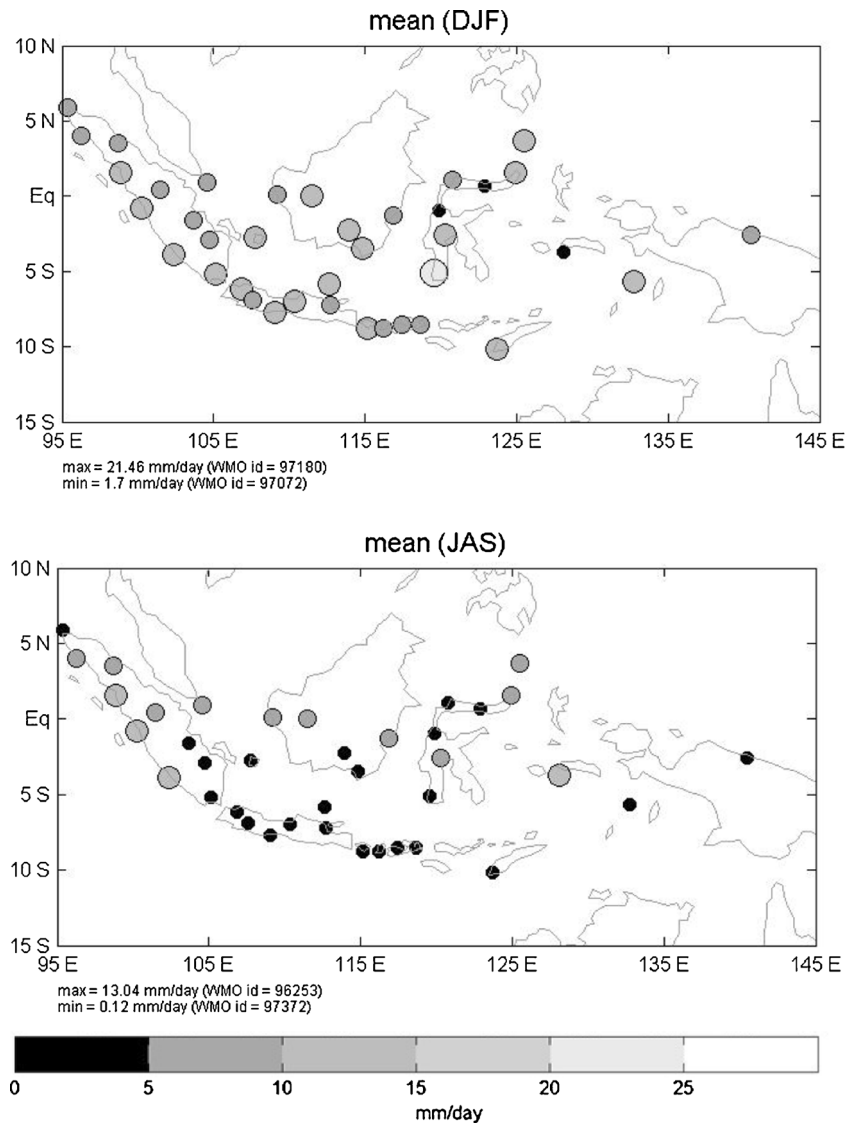




**Fig. 4** Spatial seasonal mean rainfall for active WNP monsoon (a), extreme WNP monsoon (b), active AU monsoon (c), and extreme AU monsoon (d) of 15 years (1 January 2001–31 December 2015) 3B42 data

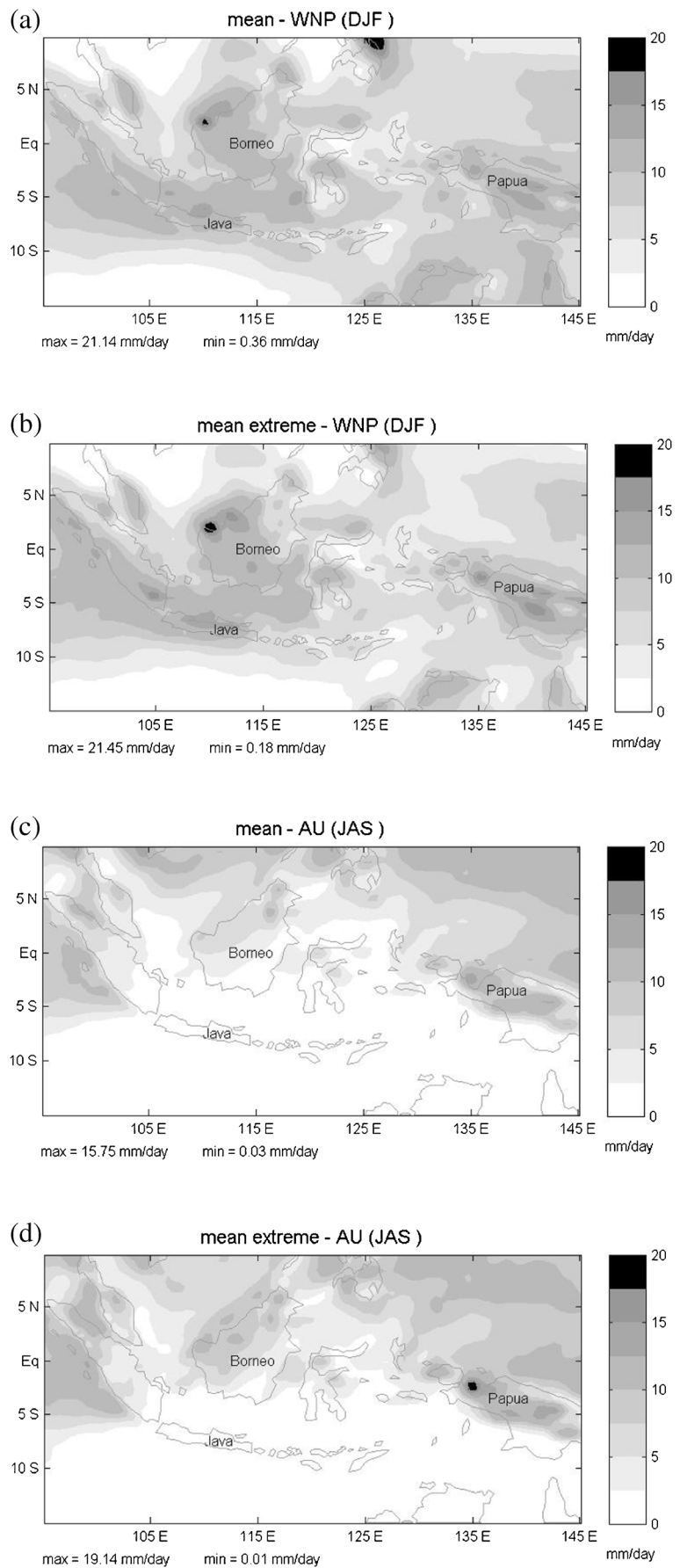
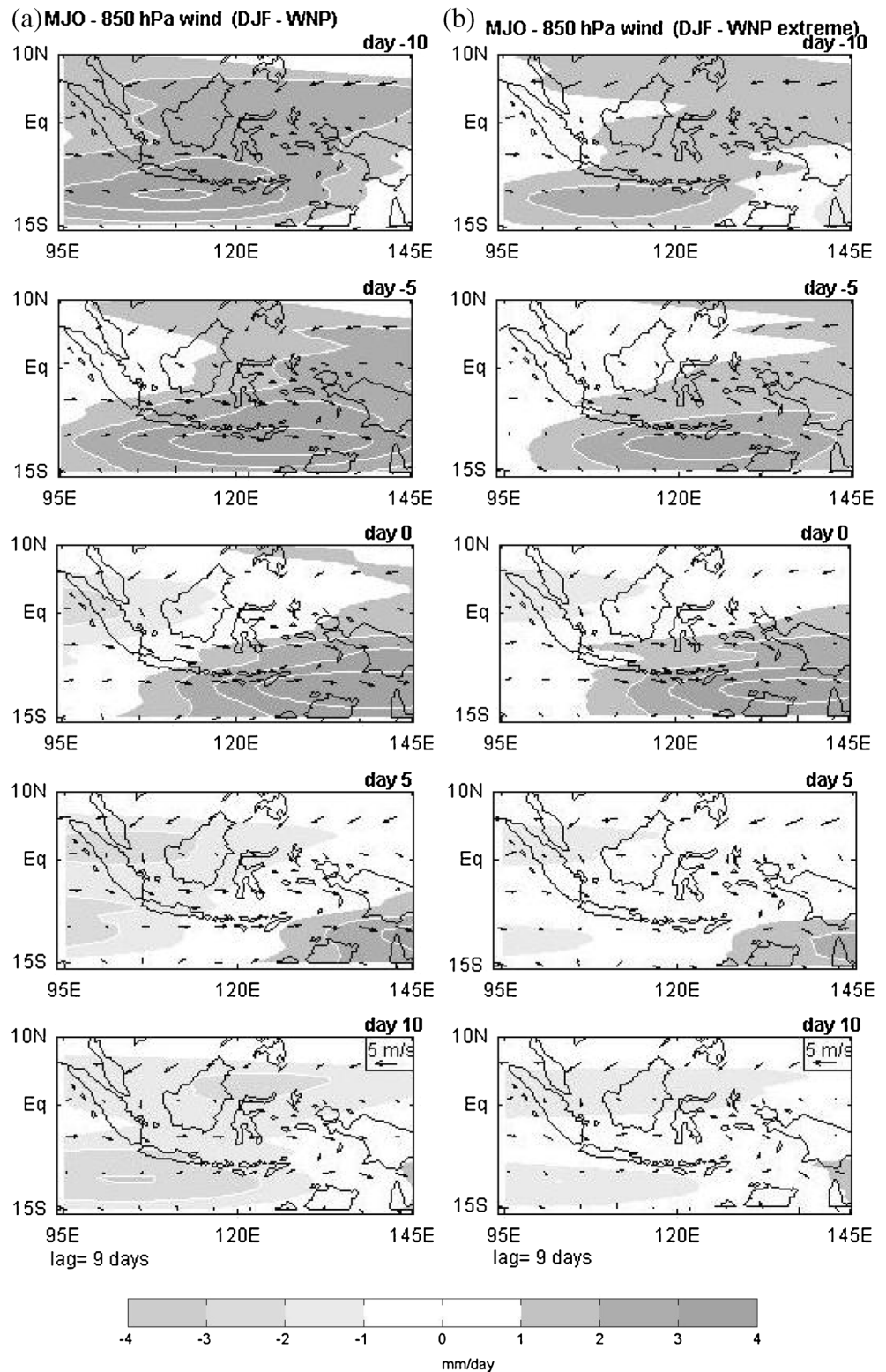


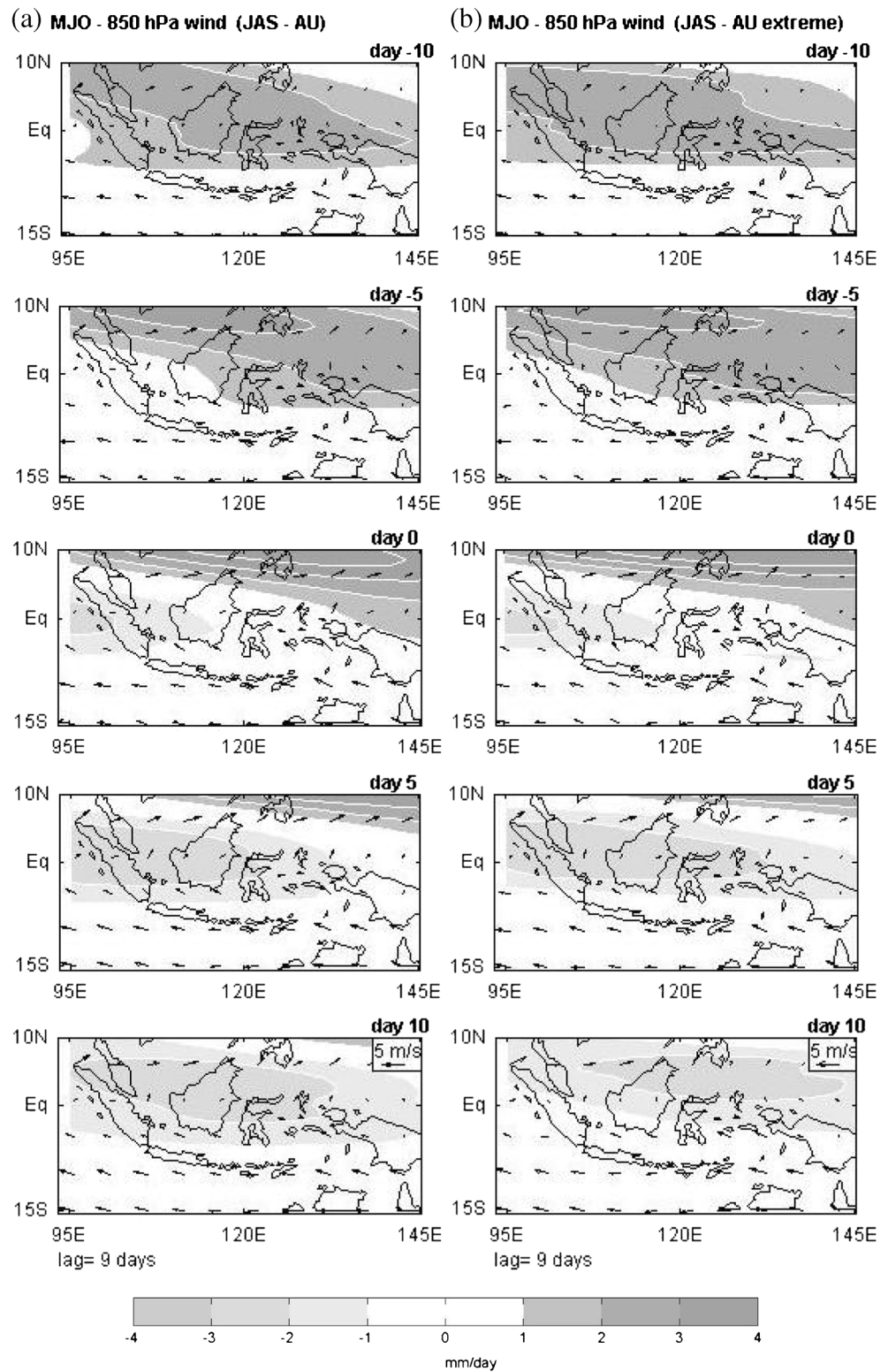
**Fig. 5** Geographical evolution for MJO refers to EOF2 using lag correlation of EOF1 and 2 from 15-year MJO-filtered TRMM-3B42 (shading area), overlaid with 15-year ERA-interim re-analysis wind at 850 hPa during DJF-WNP active monsoon (a) and DJF-WNP extreme monsoon (b)



classified into the months of both the WNP and AU monsoons. Applying the method by Wang and Fan (1999) and Yim et al. (2013), WNP indices was obtained from U850 (5–15° N, 100–130° E) to U850 (20–35° N, 110–140°

E), whereas AU indices were calculated from U850 (0–15° S, 90–130° E) to U850 (20–30° S, 100–140° E). From the calculation of each monsoon index, an extreme monsoon phase was selected to classify the months of WNP and AU

**Fig. 6** Similar with Fig. 5 but during JAS-AU active monsoon (a) and JAS-AU extreme monsoon (b)



monsoons, by choosing only the days with the positive index above its climatology (which was obtained from the average value within the same date for 30 years). The results showed that the months which are extremely positive for the AU

monsoon index were December, January, and February (DJF), whereas July, August, and September (JAS) were for the WNP monsoon index (Fig. 2). Furthermore, a simplification of naming with “monsoon name–monsoon months”



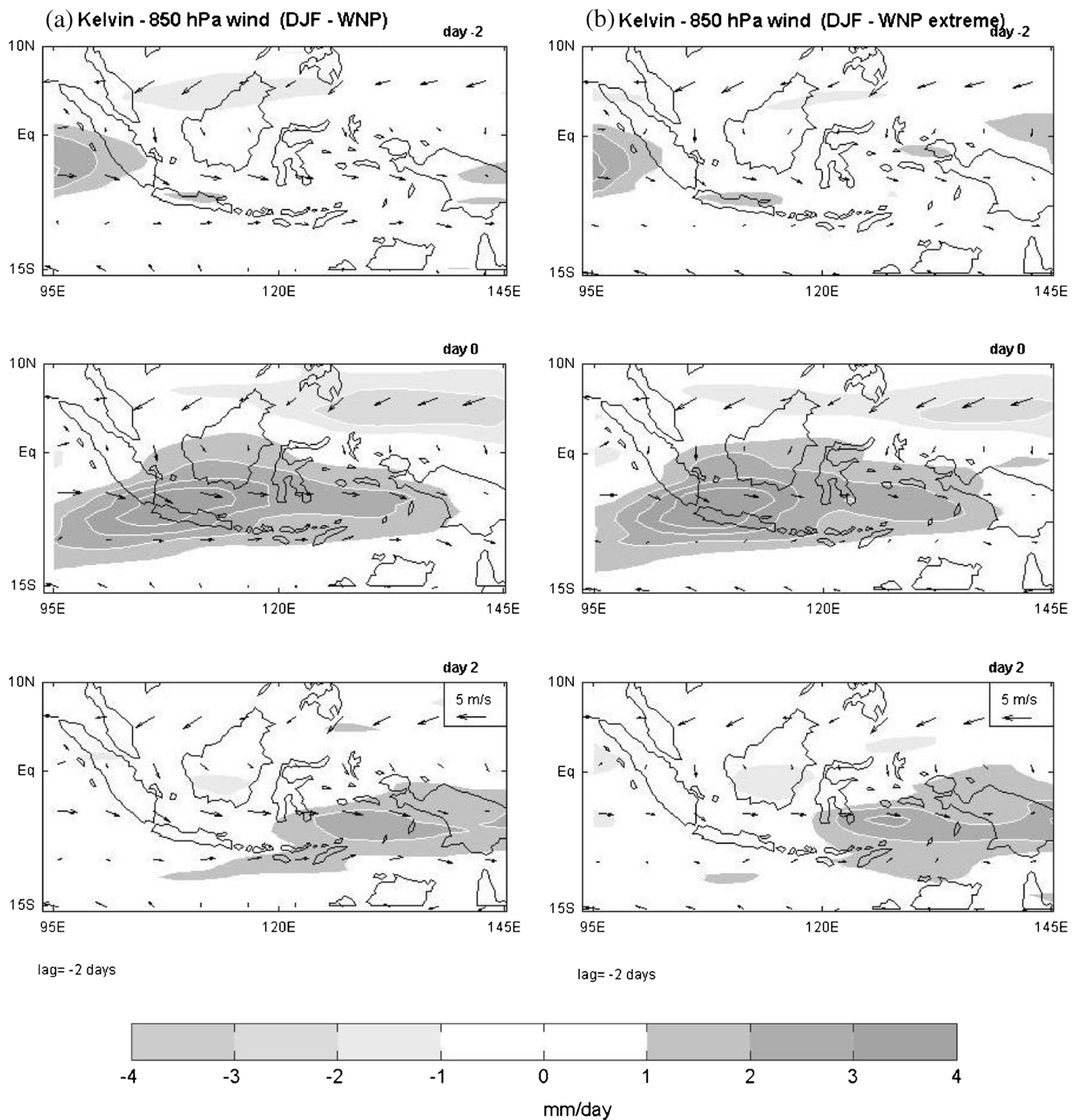


**Fig. 7** Similar with Fig. 5 but for Kelvin refers to EOF1 during DJF-WNP active monsoon (a) and DJF-WNP extreme monsoon (b)

using its abbreviation is used to represent each monsoon phase. Since, it is broadly known that naming monsoon seasons is based on the dominance of its big seasonal wind over the region rather than by its peak monsoon index, hereafter named as DJF-WNP and JAS-AU. DJF is for the WNP monsoon phase, whereas JAS is for the AU monsoon phase (dominant wind blowing from the WNP and AU regions consecutively).

The average daily rainfall from 38 synoptic stations was calculated and plotted for both DJF and JAS periods to exhibit any geographical rainfall distribution patterns during the WNP monsoon and AU monsoon phases. Figure 3 shows that during the WNP monsoon period, most of the Indonesian region experienced a peak rainfall activity, even though three stations (located in northern Sulawesi and southern Maluku) experienced a dry phase.

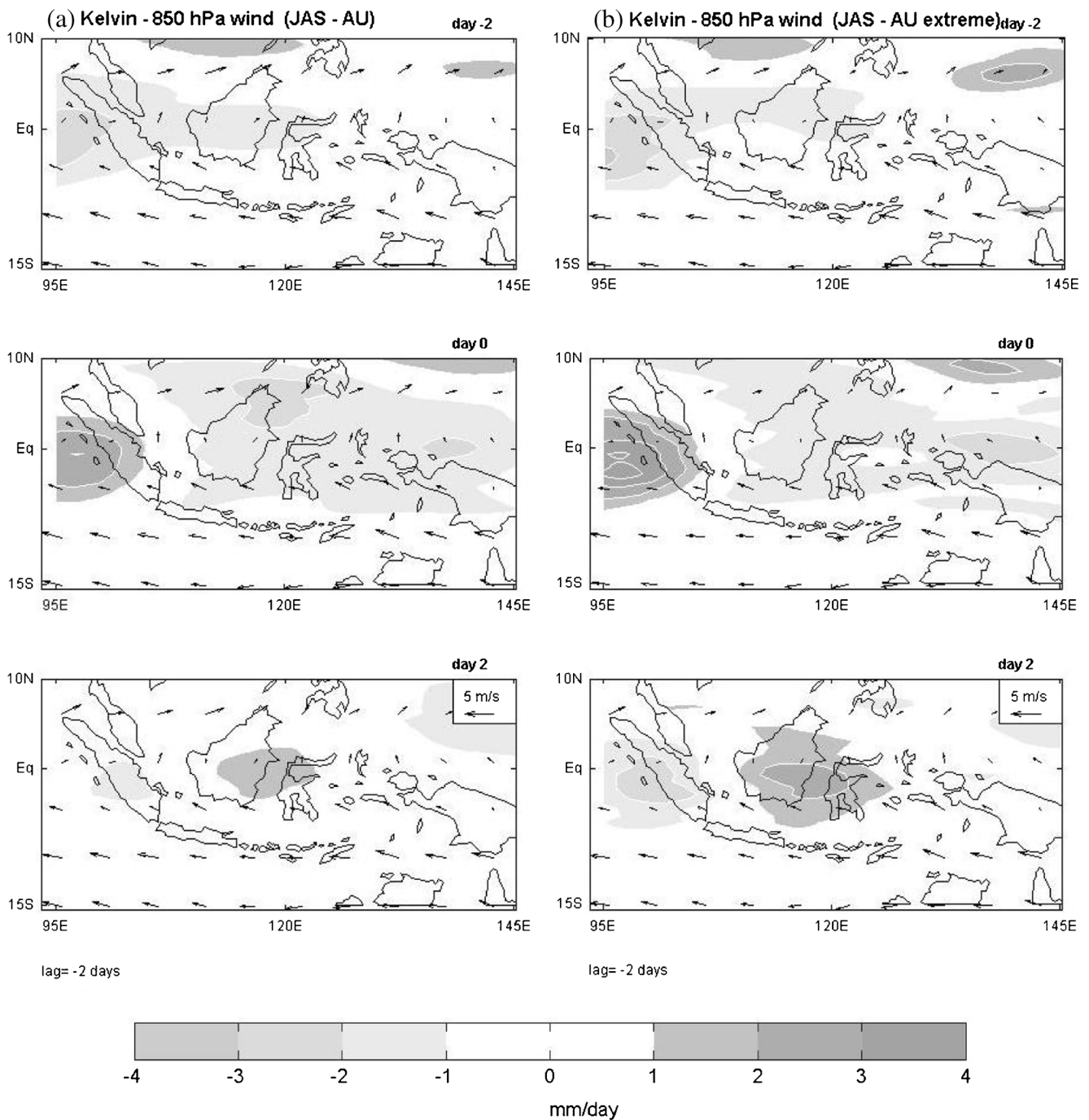


**Fig. 8** Similar with Fig. 5 but for Kelvin during JAS-AU active monsoon (a) and JAS-AU extreme monsoon (b)

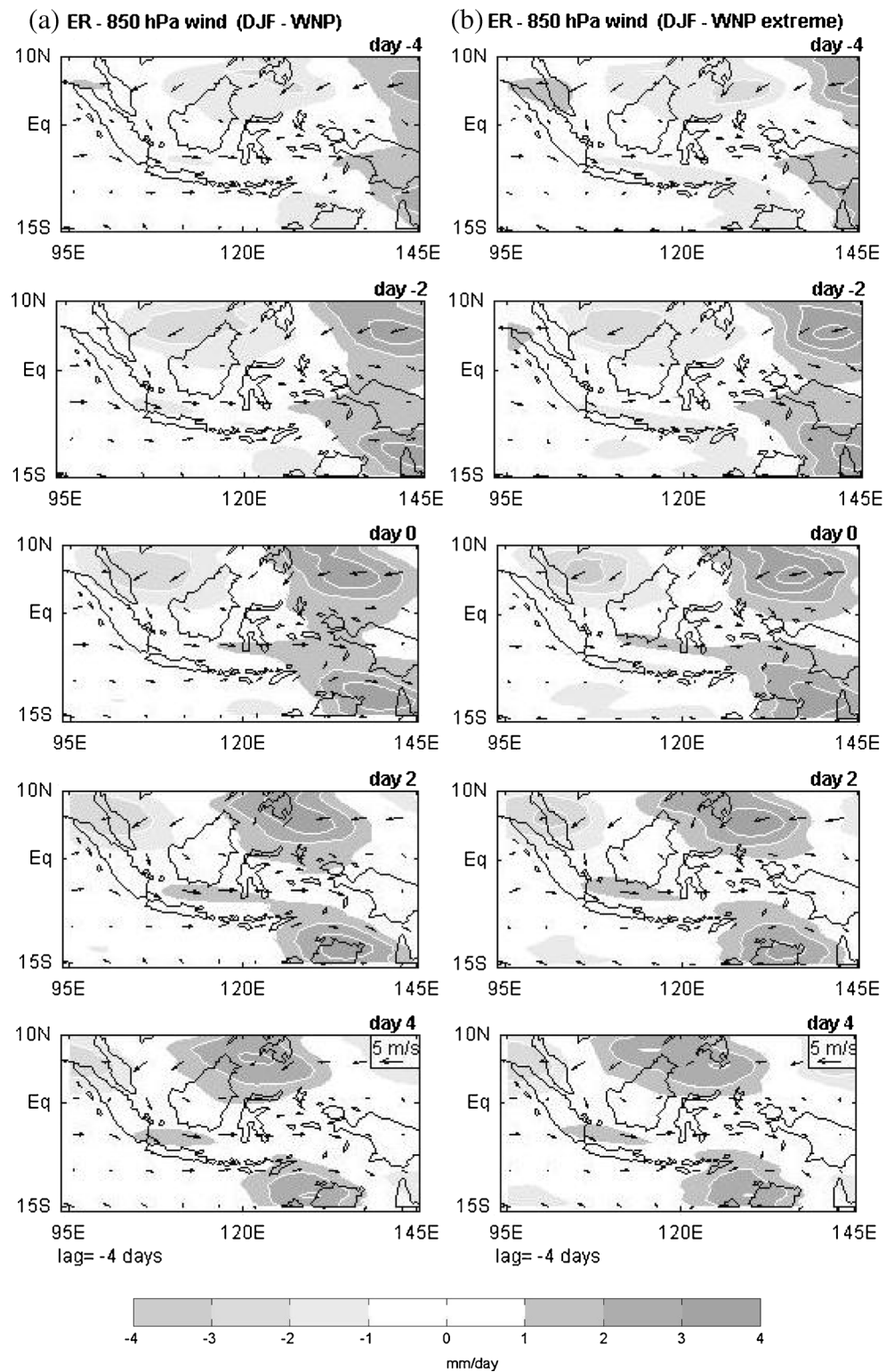
On the other hand, most of the Indonesian region such as north and south Sumatera, Java, Bali and Nusa Tenggara, South Borneo, most parts of Sulawesi, southeast Maluku Island, and most parts of Papua suffered a dry phase during the AU monsoon period, while the remaining areas encountered a peak rainy period. This condition confirms the previous study by Aldrian and Susanto (2003). Furthermore, the results denote that the WNP monsoon

during DJF represents rainy season over Indonesia, while the AU monsoon during JAS represents dry season for the most part of Indonesia.

After the WNP and AU months were classified, a certain time of active monsoon indices and extreme monsoon indices for both monsoon months were determined. Figure 4 shows a spatial daily rainfall distribution for certain times of WNP and AU active and extreme monsoon phases for 15 years. It



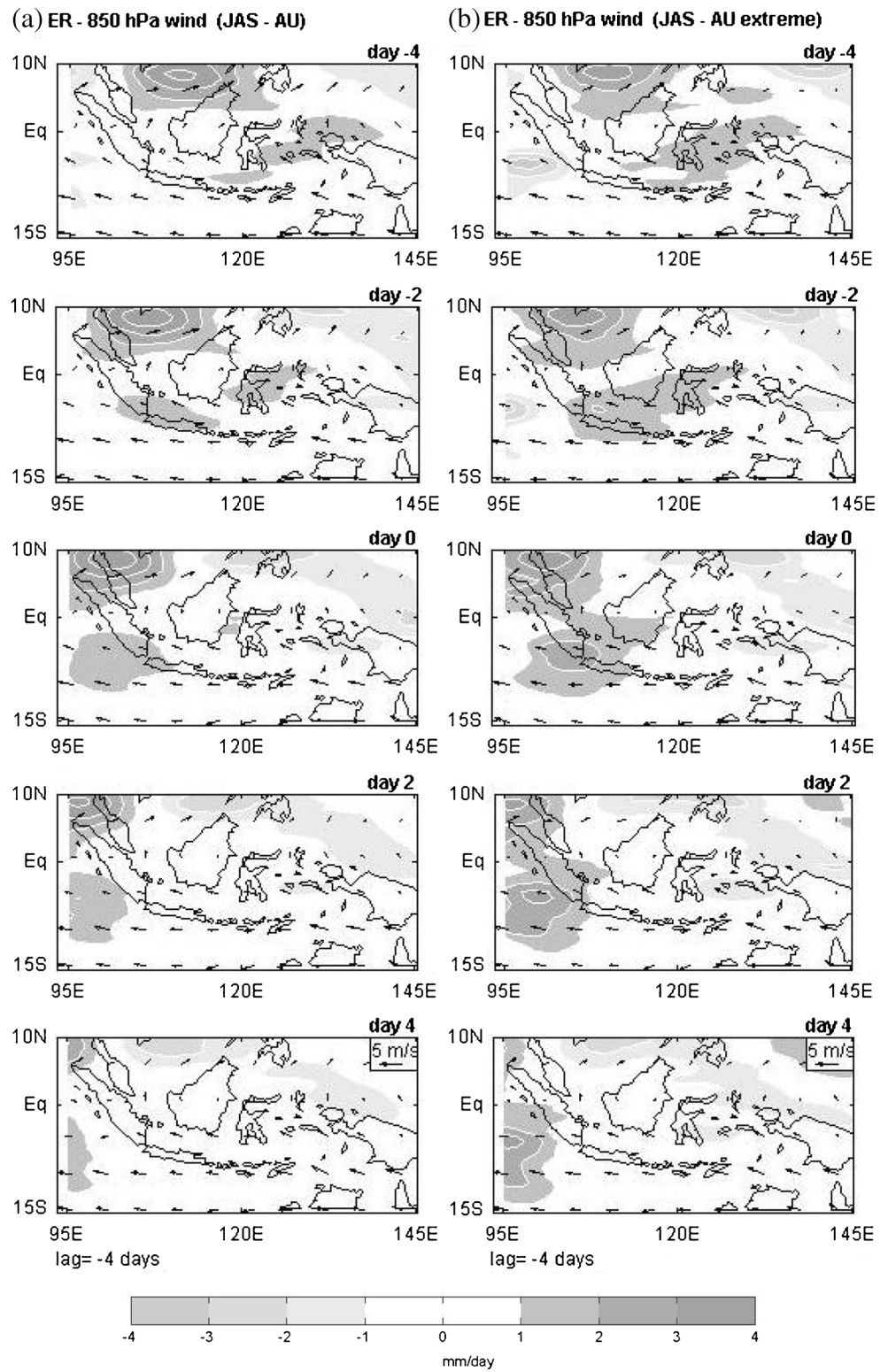
**Fig. 9** Similar with Fig. 5 but for ER refers to EOF1 during DJF-WNP active monsoon (a) and DJF-WNP extreme monsoon (b)



indicates that the rainfall is concentrated northerly during the AU active and extreme monsoon (JAS), whereas located more dispersed to the equator during WNP active and extreme monsoon (DJF). There is no significant discrepancy between

active and extreme monsoon phases, with the exception of the decrement of a daily rainfall on the south of the Philippines during the extreme WNP monsoon. It is presumably due to the cyclonic activity (i.e., tropical cyclone) in this

**Fig. 10** Similar with Fig. 5 but for ER refers to EOF1 during JAS-AU active monsoon (a) and JAS-AU extreme monsoon (b)



region, which is absent during extreme WNP monsoon, yet reached its peak during AU monsoon phase in the months of JAS, which agrees with the previous study by Lodangco and Leslie (2016). Another slight discrepancy is observed in west

Borneo, where an average of daily rainfall has slightly increased during the extreme WNP phase, which is presumably due to an enhancement of Borneo vortex activity during the extreme WNP monsoon (cf. Koseki et al. 2014). Meanwhile,

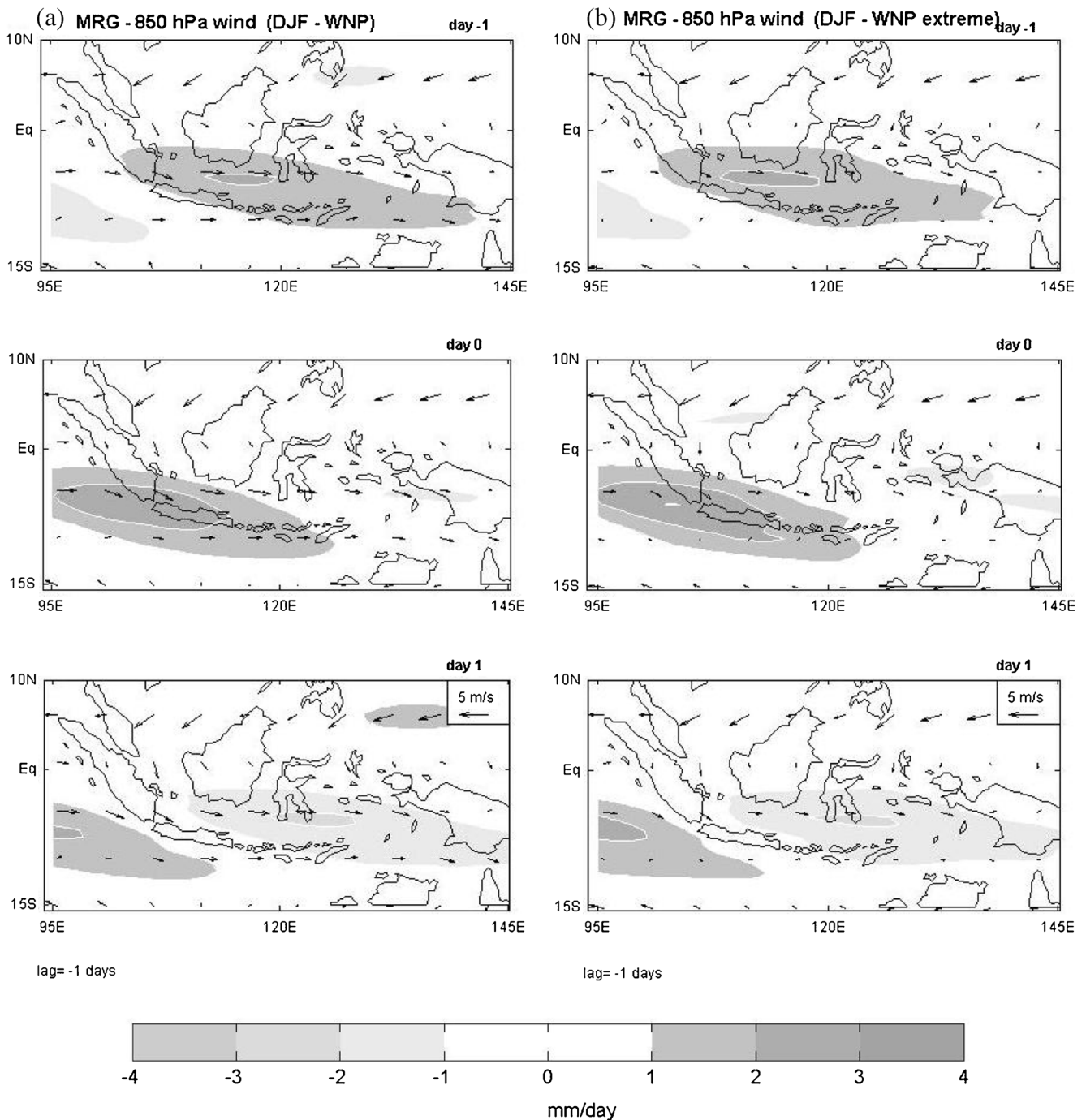


**Fig. 11** Similar with Fig. 5 but for MRG refers to EOF1 during DJF-WNP active monsoon (a) and DJF-WNP extreme monsoon (b)

the average daily rainfall increased in the extreme AU monsoon in Biak (north Papua). Although the reasons that account for this phenomenon are unknown, the topographical features in Papua might play a role, particularly when the wind flowing from the southern hemisphere (southeast) to northern hemisphere strikes the mountains of Jayawijaya (central Papua) and crosses the strait between Papua mainland and Biak.

After, the space–time spectral analysis was employed to obtain the CCEW including the MJO in the equator, applying a method from WK99 to filter the  $0.5^\circ$  grid point of the 15-year 3B42 daily precipitation by converting the time–space domain into a wavenumber–frequency domain. The equivalent depth ( $h_e$ ) applied in this study was from 8 to 90 m, and the zonal wavenumber ( $k$ ) is between  $-20$  and  $20$  for the whole equatorial globe with a latitudinal window



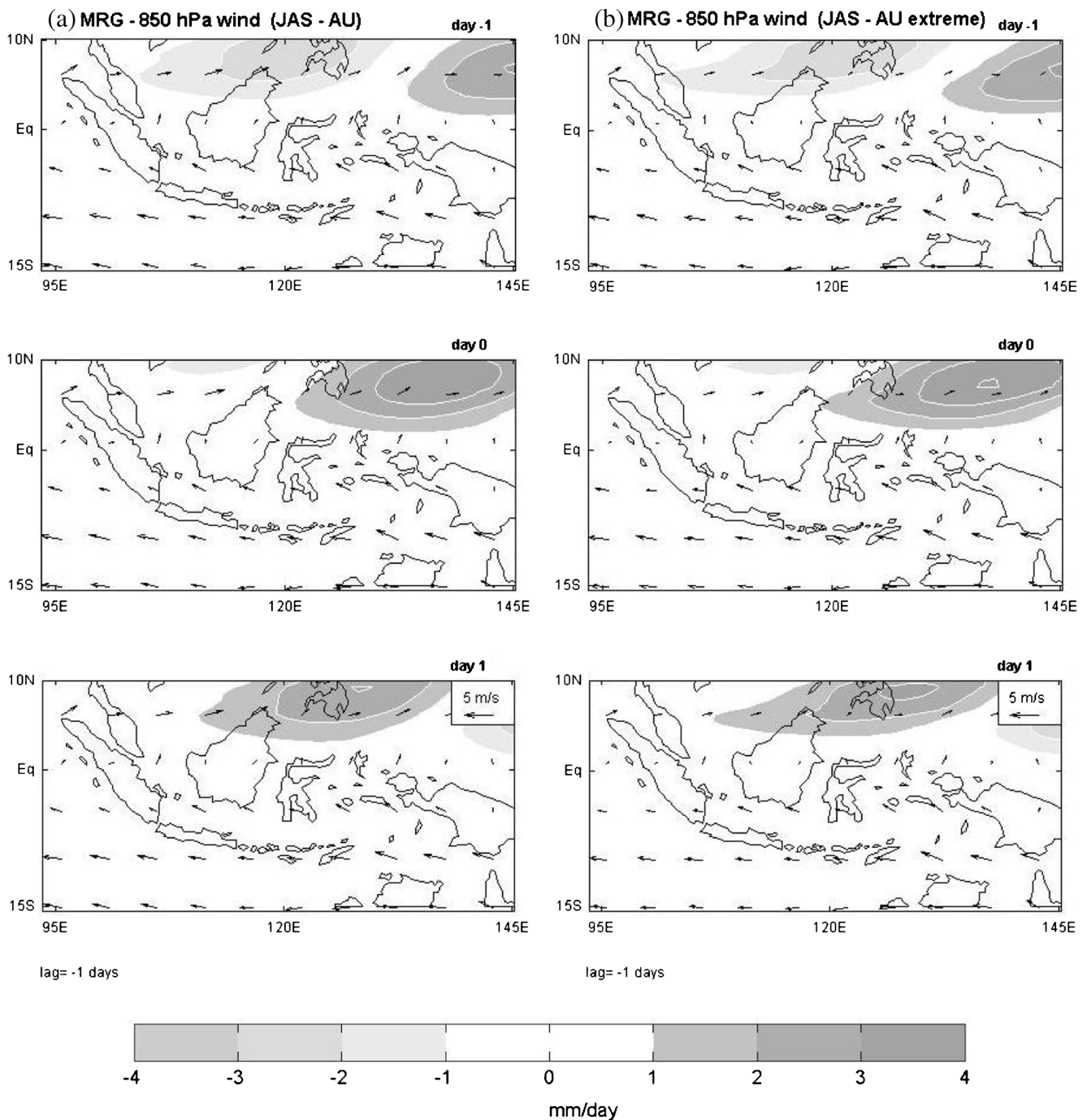


**Fig. 12** Similar with Fig. 5 but for MRG refers to EOF1 during JAS-AU active monsoon (a) and JAS-AU extreme monsoon (b)

( $\phi$ ) between 20° N and 20° S. Adapting the approach of Zhao et al. (2013), a filtered wave that resulted from the space–time spectral analysis was then calculated using the empirical orthogonal function (EOF) method to exhibit evolution. Subsequently, EOF modes 1 and 2 of the Indonesian domain were calculated to seek the peaks of the normalized unit of expansion coefficient, which are above the standard deviation. Then, they were collated into

one group of data series containing the peak events of each filtered equatorial wave. Applying the lag-correlation toward EOF modes 1 and 2, hence the time sequence and dispersion direction of each wave mode eventually gathered.

An EOF1 and 2 group data series which are obtained from the previous calculations and which coincide with the WNP and AU active and extreme monsoon phases were then plotted

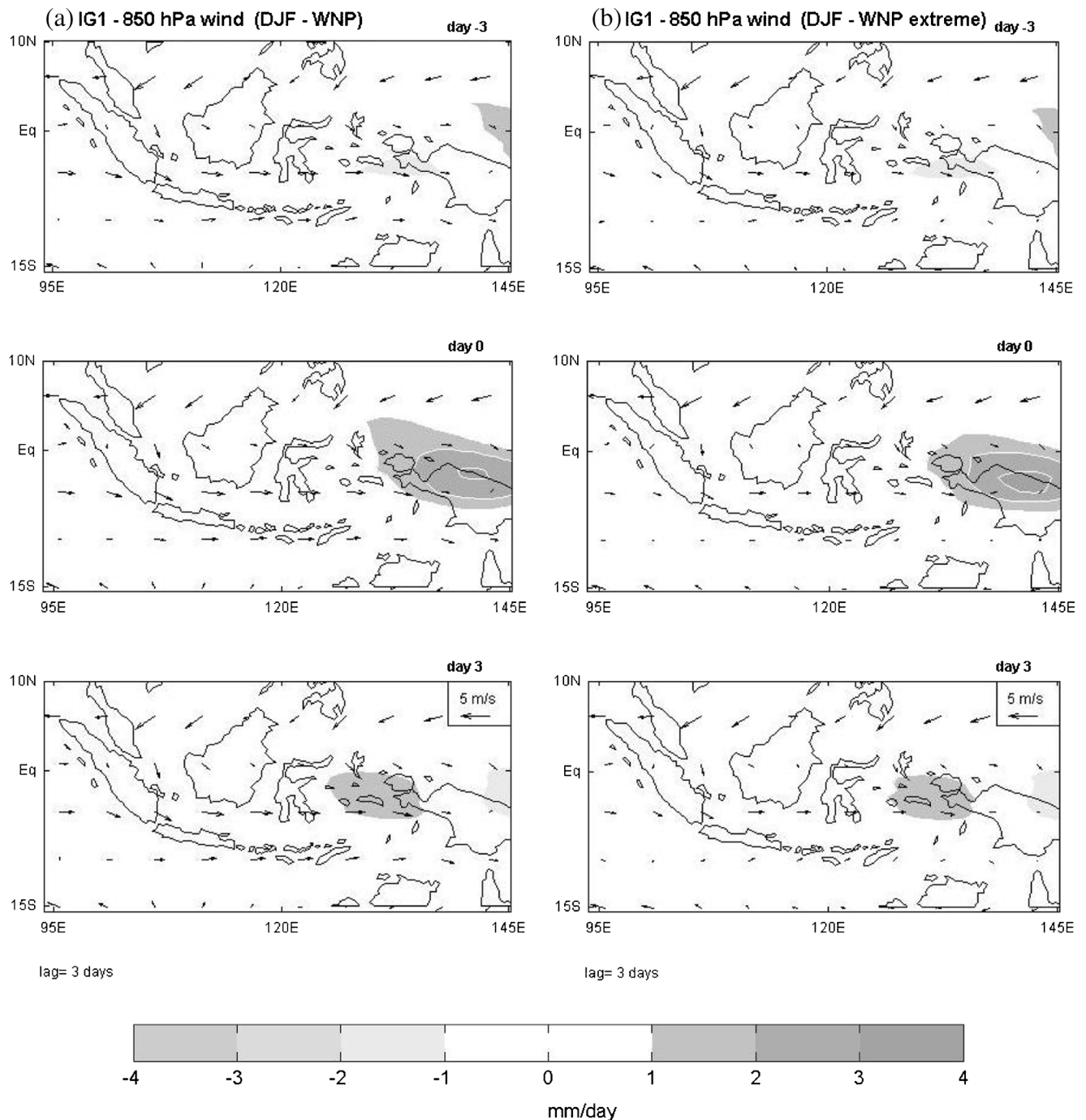


**Fig. 13** Similar with Fig. 5 but for IG1 refers to EOF1 during DJF-WNP active monsoon (a) and DJF-WNP extreme monsoon (b)

spatially. A comparison was then conducted between that spatial EOF1 and 2 against a spatial variance in the domain of Indonesia for each wave and monsoon phase. Hence, the most similar EOF with its variance was then selected, proceeding to the next calculation to represent its most appropriate evolution stage for each active and extreme monsoon phase. As a result of the EOF1 and 2 resembling with its variance (figure not shown), the MJO refers to EOF2 for both WNP and AU

monsoons, while Kelvin refers to the same mode for the AU monsoon. However, EOF1 is referenced for Kelvin during the WNP monsoon and for the rest of the waves (ER, MRG, and IG1) during both the WNP and AU monsoons. Eventually, the evolution stages from the selected EOF were calculated on these certain times to distinguish the wave's evolution during an active monsoon phase as well as during an extreme monsoon phase. The 850-hPa resultant wind within the same time



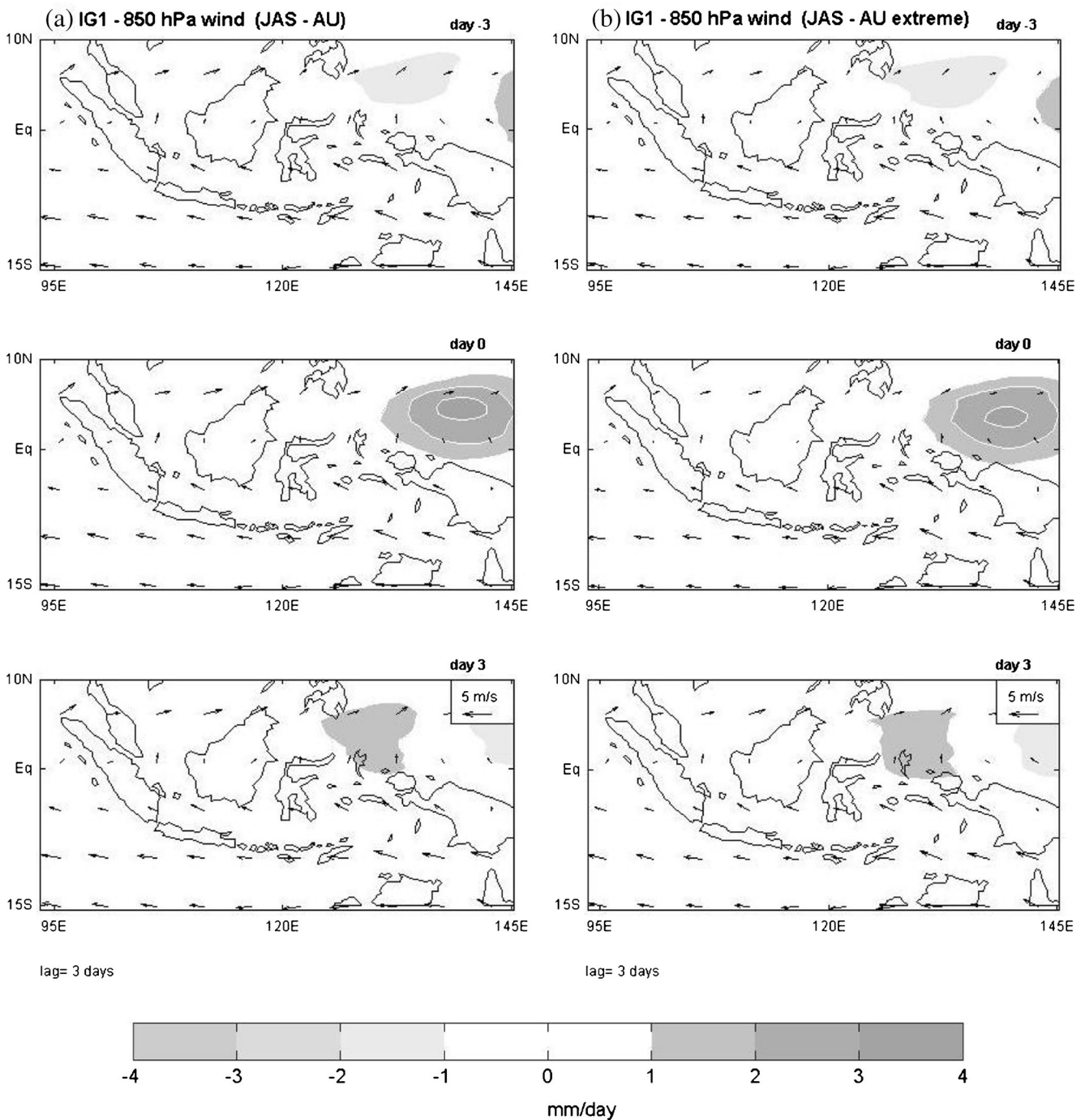


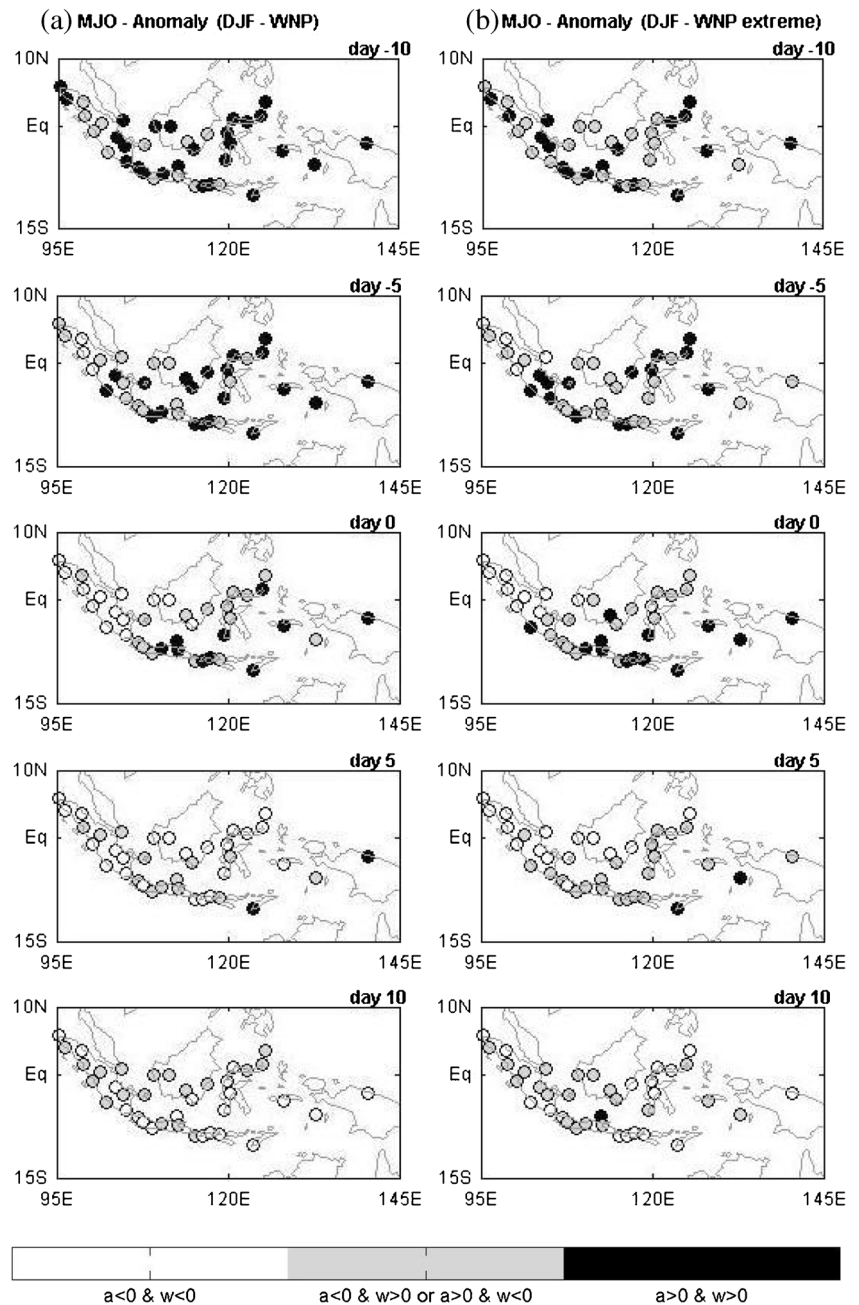
**Fig. 14** Similar with Fig.5 but for IG1 refers to EOF1 during JAS-AU active monsoon (a) and JAS-AU extreme monsoon (b)

period was then plotted to complement the low-level atmospheric dynamical condition, which will be shown in the next section.

The rainfall anomaly was then calculated climatologically (30-year period) at certain times, which was already mentioned above and for the whole 38 stations. An evolution stage for active and extreme monsoon period, explained earlier, is then juxtaposed with rainfall anomaly from 38 synoptic stations to obtain a depiction of rainfall anomaly based on

CCEW and MJO evolution over Indonesia. In order to make the result easier to understand, the classification was then divided into three categories; the first includes the stations with negative rainfall anomaly ( $a < 0$ ) during a negative wave perturbation ( $w < 0$ ) which are then assumed as a rainfall-deficiency location; the second includes the stations with negative rainfall anomaly ( $a < 0$ ) during a positive wave perturbation ( $w > 0$ ) or positive rainfall anomaly ( $a > 0$ ) during a negative wave perturbation ( $w < 0$ ) which were then assumed

**Fig. 15** Rainfall anomaly against MJO evolution stage (Fig. 5) from a 15-year rainfall observational data of 38 stations, during DJF-WNP active monsoon (a) and DJF-WNP extreme monsoon (b)



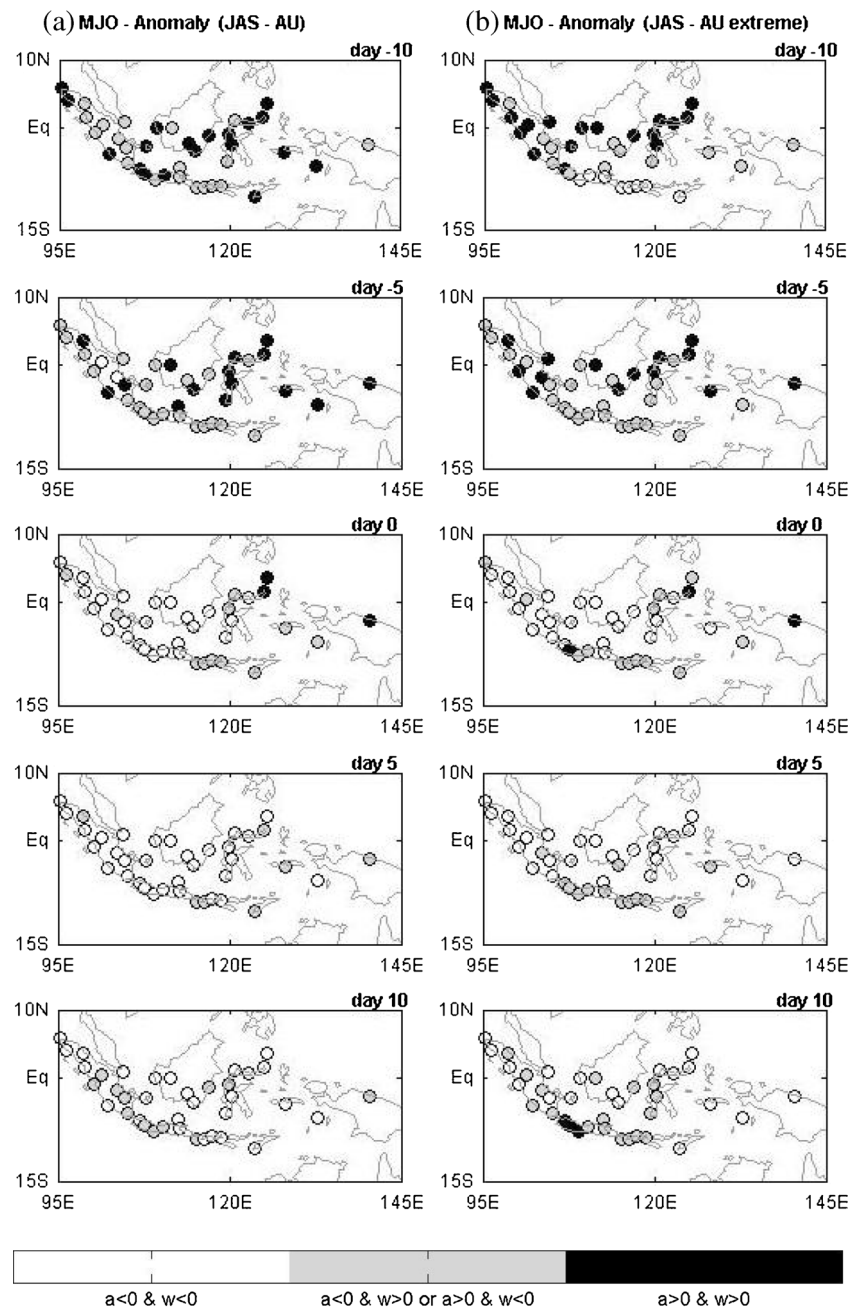
as an unrecognized relationship location, and the third includes the stations with a positive rainfall anomaly ( $a > 0$ ) during a positive wave perturbation ( $w > 0$ ) which were then assumed as a rainfall excessive location. Finally, the results of this last process will be shown in the next section.

## Results

As already described in the “Introduction” section, the final result of this study is to seek rainfall variability distribution related to the WNP and AU regional monsoon

indices in Indonesia. The geographical distribution of the CCEW and MJO evolution provides an understanding on the general behavior of each wave in Indonesia during the WNP and AU monsoon phases, which are predominant and affecting weather conditions in the region. First of all, it is important to understand the geographical distribution of CCEW and MJO evolutions which is obtained from the calculation of EOF modes 1 and 2 and from a lag-correlation analysis in the Indonesian domain (Figs. 5, 6, 7, 8, 9, 10, 11, 12, 13, and 13). Day 0 represents the day with the most vigorous variance obtained from the first or the second EOF (based on the comparison with

**Fig. 16** Similar with Fig. 15 but against MJO evolution stage (Fig. 6) during JAS-AU active monsoon (a) and JAS-AU extreme monsoon (b)



its variance, as already described in the “Methods” section) mode maxima using a back and forth technique on the subsequent day, which is derived from the lag value. The plus and minus signs on the lag values indicate the direction of wave propagations. However, these signs were neglected due to the dissimilar sign for some waves as the theories of equatorial waves have assumed. This dissimilar sign was likely caused by a large dataset that yielded a short lag.

**Geographical distribution of the CCEW and MJO evolution over Indonesia**

Figure 5a, b shows a homogeneous pattern for the MJO evolution stage for active and extreme WNP monsoon phases, except that a positive perturbation is distributed to the narrower area as well as a weaker positive perturbation strength during the extreme phase. The MJO is initiated over the Indian Ocean and propagates eastward, reaches its peak in

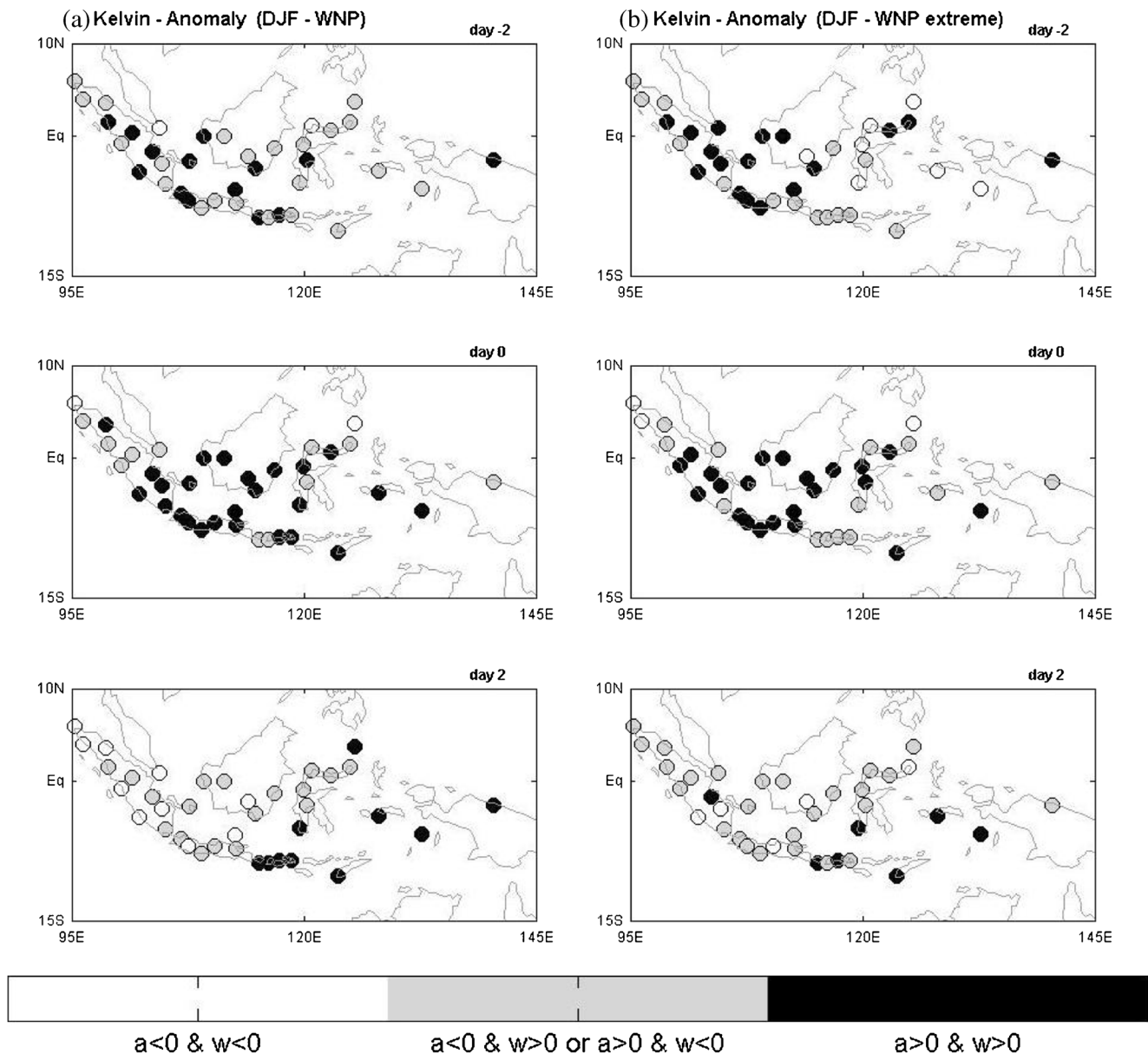


**Fig. 17** Similar with Fig. 15 but against Kelvin evolution stage (Fig. 7) during DJF-WNP active monsoon (a) and DJF-WNP extreme monsoon (b)

the Indonesia archipelago, then starts to weaken in the equatorial west Pacific Ocean, which is in line with an earlier study (Madden and Julian 1972). The positive wave perturbation mostly influences the area of the southern hemisphere of Indonesia during the DJF-WNP monsoon phase. Parallel to its propagation to the east, the negative wave perturbation follows behind, which is displaced exactly 20 days after the positive perturbation. A different pattern is shown in Fig. 6a, b for the active and extreme JAS-AU monsoon phases. The full-length positive perturbation extends from the northern hemisphere up to the equatorial line (north part of Papua), which is consistent with a previous study by Ramage (1971) and is presumably due to the monsoon flow from the Arabian

mainland. The positive perturbation shifts northward during JAS, following the solar radiation shift to the north, which also changes an affected area of disturbance to the north. Different from the affected area during DJF, the positive perturbation is restricted to the northern hemisphere. This phenomenon is presumably caused by the release of humid water vapor from Indonesia and Malaysia during the DJF-Australian summer monsoon (Ramage 1971), which later enhances the convection up to the northern hemisphere close to the equator, which is absent during JAS.

Unlike the MJO, the evolution strength of Kelvin wave during extreme monsoon in Fig. 7 exhibits a preponderant positive perturbation compared with during active Kelvin



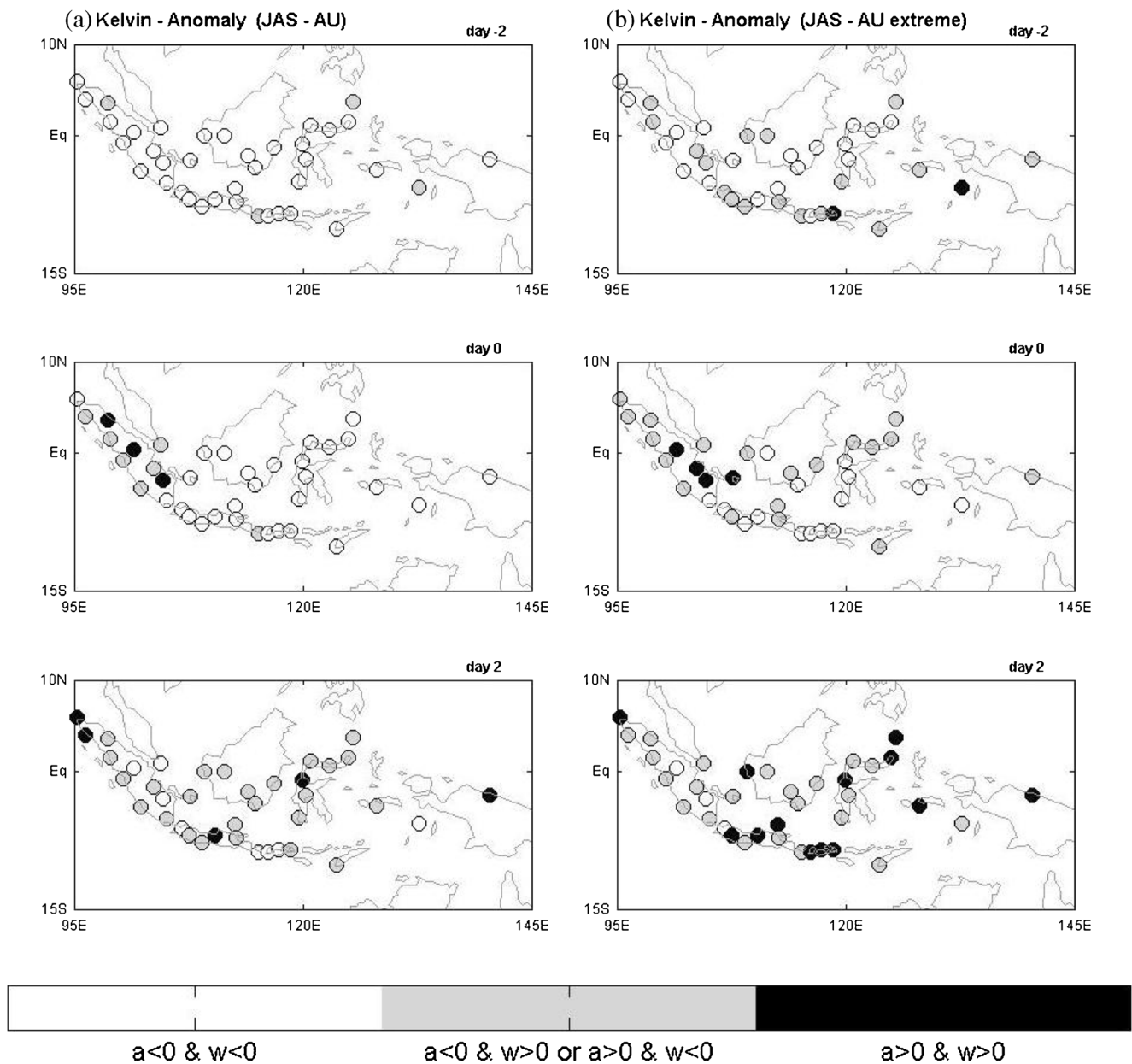


Fig. 18 Similar with Fig. 15 but against Kelvin evolution stage (Fig. 8) during JAS-AU active monsoon (a) and JAS-AU extreme monsoon (b)

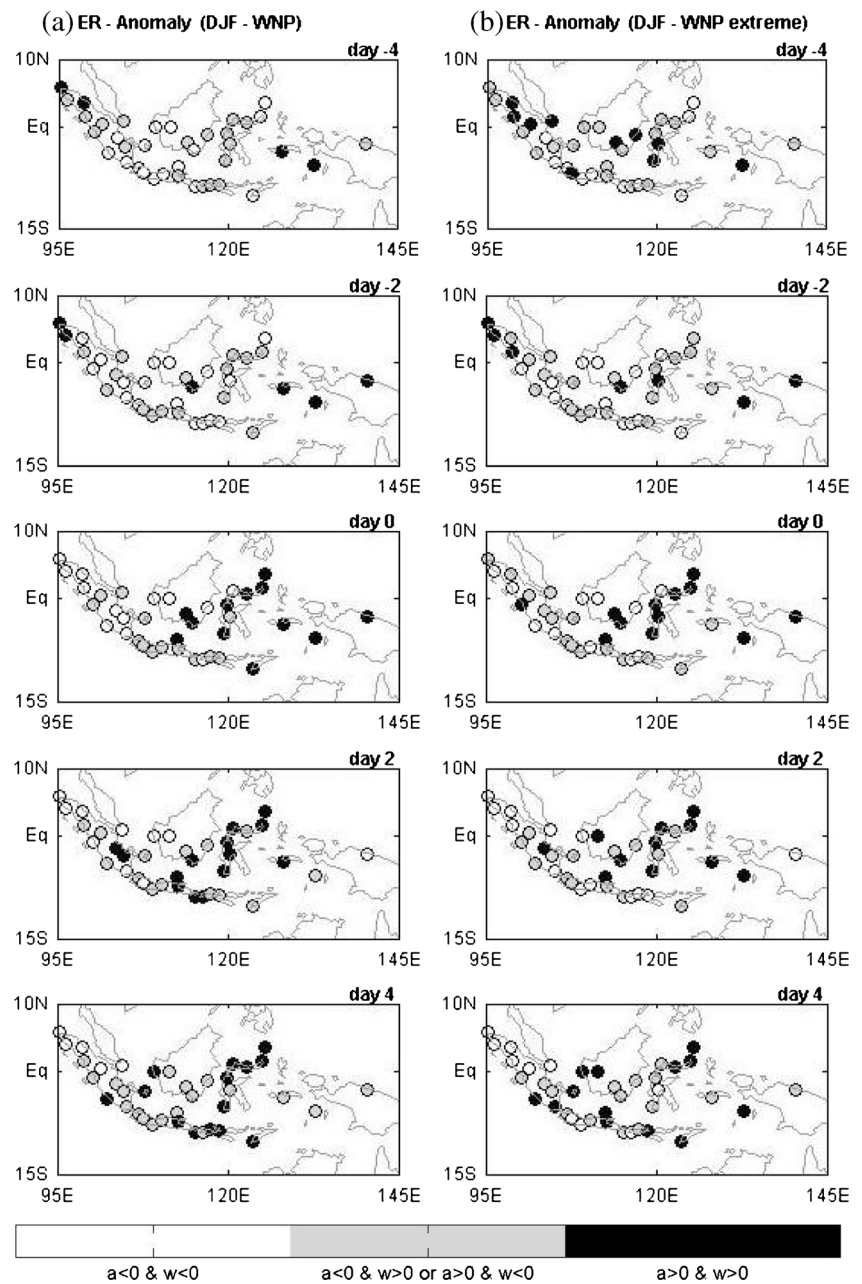
monsoon, which reached more than 4 mm/day at day 2. It means that the extreme WNP monsoon induces convective rain from Kelvin wave that is stronger than the MJO. This figure shows that the Kelvin wave entered the Indonesian region from the Indian Ocean, reached its peak mainly in the island of Java, and started to dissipate over the eastern part of Indonesia. During the JAS-AU monsoon phase (Fig. 8), the Kelvin wave that crossed Indonesia reveals a tighter positive perturbation area than during the DJF-WNP monsoon, suggesting that the Kelvin wave has triggered a convective cloud development over Indonesia at the DJF-WNP monsoon. Nevertheless, we may still recognize some similarities with

DJF-WNP, i.e., a preponderant positive perturbation during extreme monsoon compared with during active monsoon phase and confined more to the equator for both the WNP and AU monsoon phases, which will be explained later.

Dissimilar with Kelvin, ER has an opposite characteristic for impacted location (Figs. 9 and 10), where ER has an off-equatorial positive perturbation distribution both to the north and to the south during DJF-WNP and JAS-AU, even though being more bound to the off-equatorial northern hemisphere, which is also in coherence with a previous study by Lubis and Jacobi (2014). This is why the convective rain areas related to ER mostly lie in the northern and



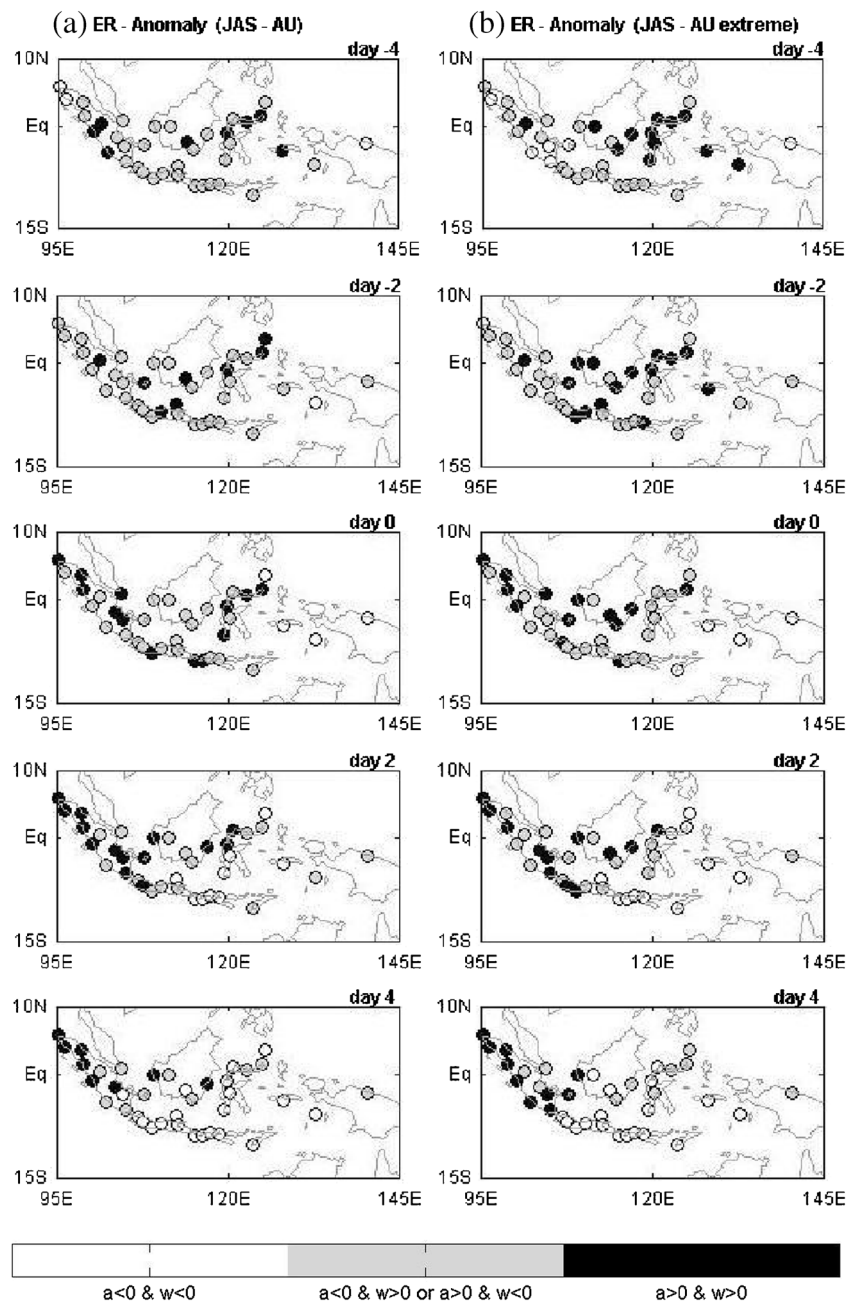
**Fig. 19** Similar with Fig. 15 but against ER evolution stage (Fig. 9) during DJF-WNP active monsoon (a) and DJF-WNP extreme monsoon (b)



southern boundaries of the Indonesian archipelago (southern part of Papua and northern part of Sumatra, Borneo, Sulawesi, and Maluku), except south Sumatra and West Java at Day 0 during JAS-AU extreme monsoon. Similar with Kelvin, ER also exhibits a preponderant positive perturbation during an extreme monsoon compared with during an active monsoon phase for both DJF-WNP and JAS-AU monsoon phases. The results that showed a pair of positive (negative) perturbations structure that are sequentially parallel to the equator in Figs. 9 and 10 are also consistent with the theory proposed by Matsuno (1966) and Kiladis et al. (2009) for  $n = 1$  ER.

Figures 11 and 12 show that MRG triggers a convective rain development during the DJF-WNP monsoon phase over south Sumatra and most part of Java Island, while it does not give any impact during JAS-AU monsoon phases. Nevertheless, although distinct from the positive perturbation that appears during the DJF-WNP monsoon that reflects a convective development in the area, this presumably could be neglected due to a weaker value of its wave perturbation, compared with the previous waves. This is indicated by a robust perturbation (3–4 mm/day) in the equatorial western Pacific north of Papua during JAS, which presumably originated from the equatorial central Pacific that flows toward the

**Fig. 20** Similar with Fig. 15 but against ER evolution stage (Fig. 10) during JAS-AU active monsoon (a) and JAS-AU extreme monsoon (b)



Philippines (Kiladis et al. 2009). Thus, the positive signal in the southern hemisphere during DJF-WNP has no significant meaning compared with the ones in the northern hemisphere during JAS-AU.

Meanwhile, IG1 indicates a peak perturbation signal in the eastern part of the Indonesian archipelago (i.e., north Maluku Island and Papua) for both DJF-WNP and JAS-AU monsoon phase (Figs. 13 and 14), as noted by previous studies (e.g., Wheeler and Kiladis 1999; Kiladis et al. 2009). Similar to Kelvin and ER, IG1 also indicates a prominent strengthening convective rain activity during an extreme monsoon

compared with during an active monsoon phase particularly at DJF-WNP over central-north Papua. However, similar to Kelvin, this IG1 wave is also confined more to the equator (Matsuno 1966; Gill 1982) despite being bounded toward the northern hemisphere near the equatorial line during the JAS-AU monsoon phase.

### Rainfall variability distribution over Indonesia

The variability of rainfall anomaly related to the MJO development during DJF-WNP seems to follow a positive

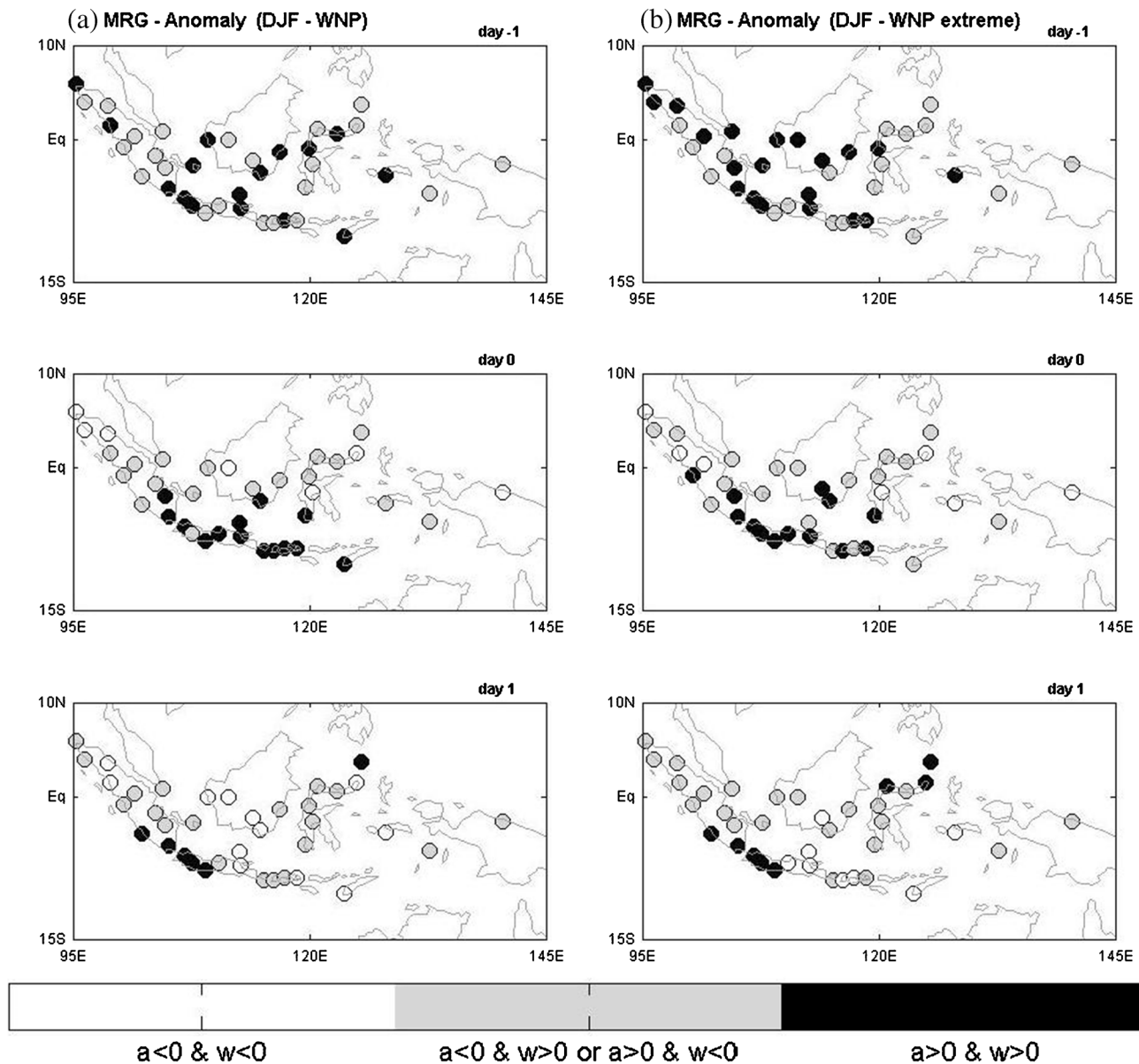


Fig. 21 Similar with Fig. 15 but against MRG evolution stage (Fig. 11) during DJF-WNP active monsoon (a) and DJF-WNP extreme monsoon (b)

(negative) perturbation signal which indicates an increasing (decreasing) rainfall activity over the shading area (Fig. 15). A positive anomaly was exhibited during Day -10 up to Day 0 over the central to eastern part of Indonesia. While an undefined relationship between the MJO perturbation sign and rainfall anomaly is likely due to other local factors that dominate in the region since the Indonesian archipelago has a complex topography. Meanwhile, a northern increasing convective rain development from Day -10 to -5, and some areas at Day 0 (Fig. 16) indicate a similarity with what is shown in Fig. 15, except for its being northerly bound compared with during DJF-WNP. At Day 10 during the JAS-AU extreme monsoon, three stations are still retained in West Java

with increasing rainfall activity due to the MJO perturbation, which implies that the JAS-AU extreme monsoon phase has given a significant effect to enhancing convection development in those regions. This result suggests that rainfall variability over Indonesia is significantly driven by deep convection associated with the MJO, which is parallel to what is already pointed out by Hidayat and Kizu (2010).

Figure 17 shows that the Kelvin wave has given a significant impact in increasing rainfall activity during both active and extreme DJF-WNP monsoon phase as revealed by Kiladis et al. (2009) and Horinouchi (2012), particularly at Day 0. The areas with a predominant positive wave perturbation that are covered by convective rain are south Sumatera, mostly Java

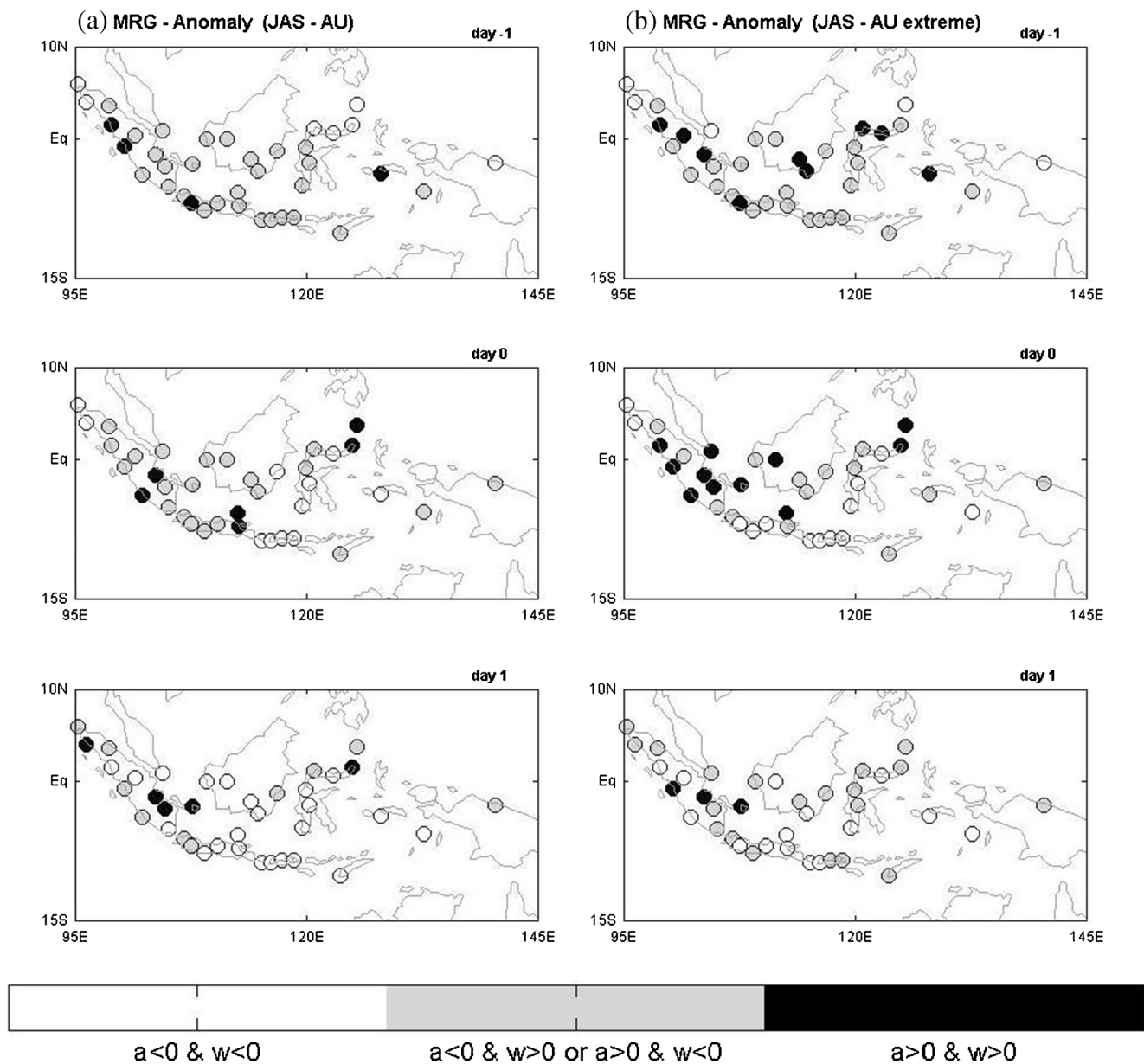


Fig. 22 Similar with Fig. 15 but against MRG evolution stage (Fig. 12) during JAS-AU active monsoon (a) and JAS-AU extreme monsoon (b)

and south Borneo. Meanwhile, during the JAS-AU monsoon phase (Fig. 18), a negative wave perturbation successfully decreases the development of rain clouds, particularly for active monsoon phase at Day -2 up to Day 0. However, a significant positive Kelvin perturbation at Day 2 over east Borneo and central Sulawesi (Fig. 8) has not been able to intensify rainfall activity in those areas.

Figures 19 and 20 show a disorganized distribution of ER wave-rainfall anomaly relationship, although some areas still indicate a positive relationship. One of which is the northern part of Sulawesi during both an active and extreme DJF-WNP monsoon phase particularly at Day 0 until Day 4 (Fig. 19). Nevertheless, the area with an increasing rainfall in Fig. 20

also exhibited over the most part of Sumatera at Day 0 until Day 4 during the JAS-AU monsoon phase, which follows the positive ER perturbation over this area. This increasing wave-rainfall anomaly area is presumably induced by a remaining of ER southern hemisphere pair structure, which is in line with what has already been described based on the theories discussed earlier by Matsuno (1966) and Kiladis et al. (2009). Meanwhile, the rainfall decrement has been apparent over north Sumatera during the DJF-WNP monsoon from Day 0 to Day 4 (Fig. 19), which coincides with the negative ER perturbation crossing this area (Fig. 9).

Although, the distinct positive MRG perturbation that appears over Indonesia during DJF-WNP could apparently be



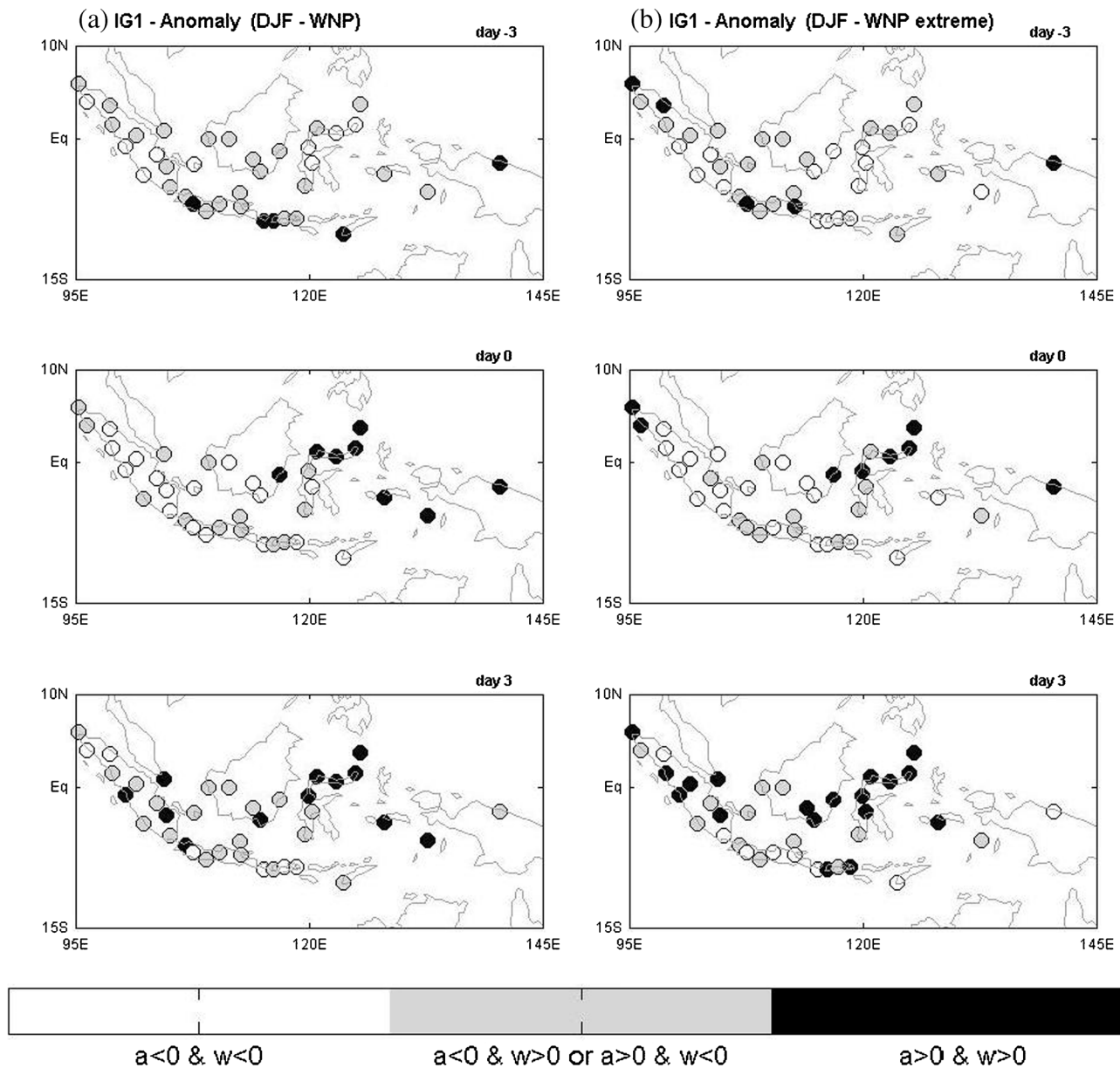


**Fig. 23** Similar with Fig. 15 but against IG1 evolution stage (Fig. 13) during DJF-WNP active monsoon (a) and DJF-WNP extreme monsoon (b)

neglected due to a weaker magnitude of wave perturbation (Fig. 11) compared with previous waves, in fact, the areas of positive MRG perturbation reflect a strong relationship in enhancing rainfall activity. Figure 21 exhibits the predominant positive rainfall anomaly where focused over south Sumatera and Java Island at Day 0 and weaken over south Sumatera and western Java at Day -1 and Day 1 during DJF-WNP monsoon phase. Meanwhile, Fig. 22 shows an absence of impacted area by MRG during both an active and extreme JAS-AU phase. Therefore, the MRG wave-rainfall anomaly relationship during this phase could be neglected. Even though some areas exhibit coherence in

positive or negative for wave perturbation and rainfall anomaly, yet the distribution shows an unorganized pattern, which may be caused by other local-scale factors. However, a stronger correlation of MRG wave-rainfall anomaly relationship during DJF-WNP exhibits a new distinctness referred from the previous study by Kiladis et al. (2009) and Horinouchi (2012) or rather being ignored considering what has been mentioned beforehand in this first line.

According to previous studies by Wheeler and Kiladis (1999) and Kiladis et al. (2009) and with what has already been described above, IG1 has given a dominant impact over Papua, which is also shown in Figs. 23 and 24. Another area



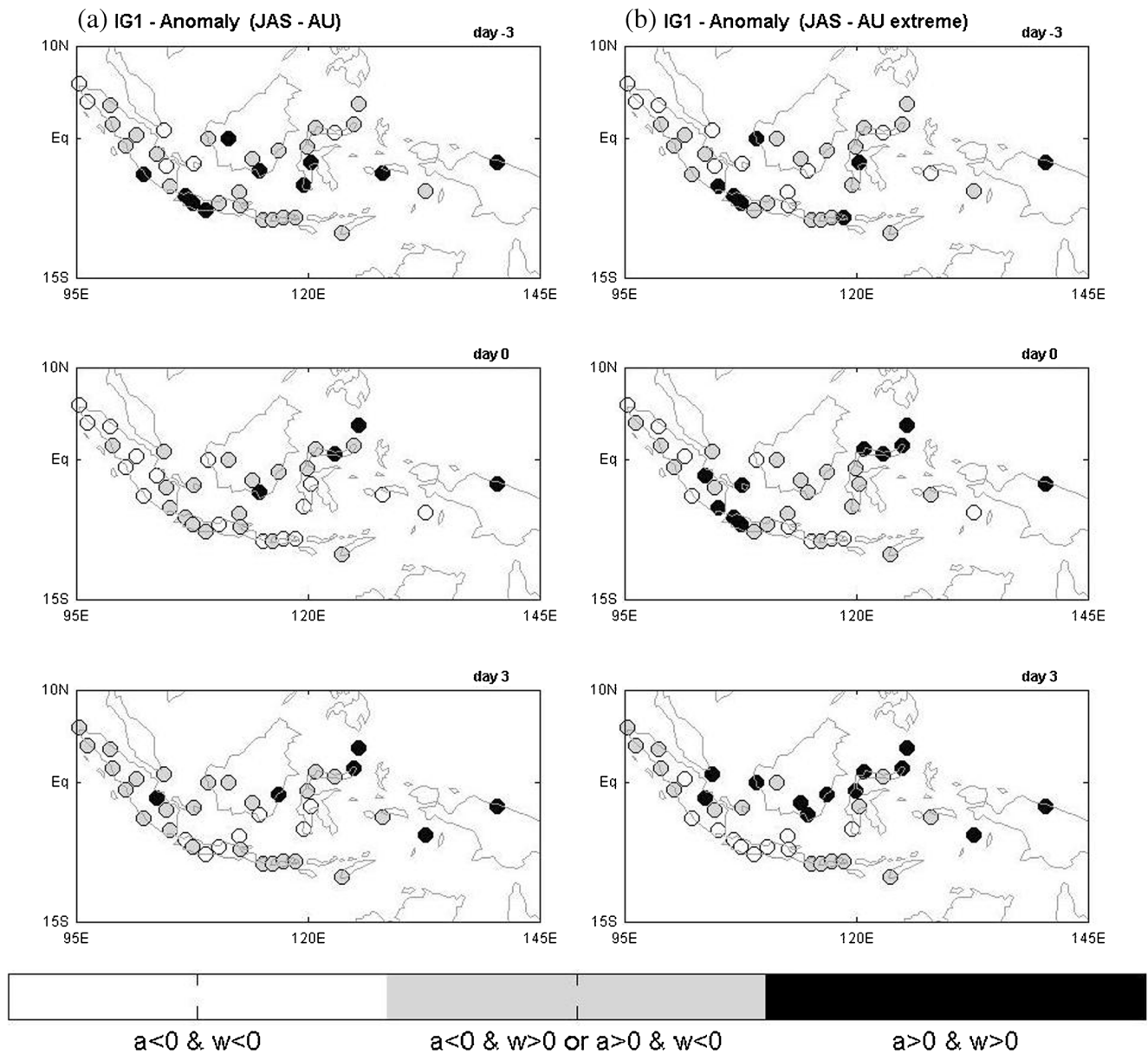


Fig. 24 Similar with Fig. 15 but against IG1 evolution stage (Fig. 14) during JAS-AU active monsoon (a) and JAS-AU extreme monsoon (b)

that has a significant positive rainfall anomaly–wave perturbation relation during active and extreme monsoon phases for both DJF-WNP and JAS-AU is north Sulawesi, even

though the positive IG1 perturbation values in Figs. 13 and 14 are not too significant. Rainfall reduction impact related to negative IG1 perturbation seems to be not clearly

**Table 1** Percentage of negative and positive wave–rainfall anomaly relation considered for monsoon phase classification

	All value (%)		Sig. value (%)	
	Pos (+)	Neg (-)	Pos (+)	Neg (-)
Active monsoon phase				
DJF-WNP	55.82	44.18	69.17	30.83
JAS-AU	54.16	45.84	69.71	30.29
Extreme monsoon phase				
DJF-WNP	54.71	45.29	60.66	39.34
JAS-AU	53.32	46.68	59.52	40.48

**Table 2** Percentage of negative and positive wave–rainfall anomaly relation considered for evolution day classification

	Active (%)		Extreme (%)	
	Pos (+)	Neg (–)	Pos (+)	Neg (–)
All value				
Day 1st	48.16	51.84	52.37	47.63
Day 0	61.32	38.68	58.42	41.58
Day end	53.42	46.58	52.63	47.37
Significance value				
Day 1st	64.49	35.51	55.45	44.55
Day 0	80.91	19.09	67.19	32.81
Day end	62.77	37.23	50.00	50.00

identified, which is presumably due to a lack of negative wave perturbation area that lied over the region of Indonesia (Figs. 13 and 14).

Percentage tables were made to ease the understanding of wave and rainfall anomaly relationships based on three classifications, i.e., Table 1 for monsoon phase classification, Table 2 for evolution day classification and Table 3 for wave's type classification. Positive (Pos) relation was obtained by calculating an equal wave–rainfall anomaly value, i.e., positive wave perturbation against positive rainfall anomaly as well as negative wave perturbation against negative rainfall anomaly, whereas negative (Neg) relationship was obtained by calculating a non-equal wave–rainfall anomaly value, i.e., positive (negative) wave perturbation against negative (positive) rainfall anomaly. Meanwhile,

**Table 3** Percentage of negative and positive wave–rainfall anomaly relation considered for wave-type classification

	Active (%)		Extreme (%)	
	Pos (+)	Neg (–)	Pos (+)	Neg (–)
All value				
MJO	62.37	37.63	54.47	45.53
Kelvin	61.84	38.16	51.32	48.68
ER	52.37	47.63	55.79	44.21
MRG	48.68	51.32	49.12	50.88
IG1	46.49	53.51	57.89	42.11
Significance value				
MJO	68.74	31.26	64.86	35.14
Kelvin	79.56	20.44	51.32	48.68
ER	62.05	37.95	60.78	39.22
MRG	58.33	41.67	78.75	21.25
IG1	100.00	0.00	100.00	0.00

considerations due to the significant wave perturbation values seem to be necessary. Therefore, we can notice how a considerably strong wave perturbation affects rainfall anomaly compared with all perturbation wave intensity that affects rainfall anomaly over Indonesia. In this classification, a wave perturbation value more than 1 mm/day or less than –1 mm/day (as shown in Figs. 5, 6, 7, 8, 9, 10, 11, 12, 13, and 14) was classified into a significant value group, whereas all value group consists of all wave without value range classification.

From Table 1, except for Sig value during all active monsoon phases, we notice that the entire Pos relationships during DJF-WNP are stronger than JAS-AU positive relationships. Wave–rainfall anomaly relationships seem to be more significant for Sig value compared with all value. Meanwhile, a slight difference (less than 1%) was exhibited for Sig value classification during all active monsoons for both the DJF-WNP and the JAS-AU monsoon phases (69.17 and 69.71%, respectively), thus we may conclude that the DJF-WNP extreme monsoon phase has given more impact toward rainfall anomaly (60.66%) particularly for a significant wave perturbation value classification. Meanwhile, Table 2 shows that wave perturbation has given the most robust impact toward rainfall anomaly at Day 0 compared with the first and the end days of wave evolution period. Even though Pos relationship at Day 1st during active monsoon for all value classification is weaker than Neg relationship (48.16 against 51.84%), other Pos relationships are stronger than Neg relationships. Overall, wave–rainfall anomaly relations are more significant for all active monsoon phases than for extreme monsoon phases, as well as stronger for Sig value classification compared with all value classification. From these findings, we can conclude that the wave–rainfall anomaly relationship is significant at Day 0 for a significant wave perturbation value and during an active monsoon over Indonesia (about 37.88% from total Day in Table 2). The wave–rainfall anomaly relationship based on wave type presented in Table 3 indicates a random conclusion, where a certain wave is significant for a certain classification, i.e., the MJO–rainfall anomaly relationship is stronger during all active monsoon phases for all wave perturbation values (62.37%); the Kelvin wave is stronger during all active monsoon phases for a significant wave perturbation value (79.56%); the ER wave is stronger during extreme monsoon phase for all value (55.79%); the MRG wave is the most significant wave during an extreme monsoon phase for a significant value (78.75%). Meanwhile, IG1 looks stronger during the extreme monsoon for all wave perturbation value classifications and during all active monsoon phases for a significant value (up to 100%). Nevertheless, due to a limited number of stations that show a positive IG1 wave–rainfall anomaly relationship (only Papua and Maluku), an exception is made for this wave that IG1 is significant to influence rainfall anomaly over east Indonesia.

## Discussion and conclusion

We have shown the rainfall variability distribution based on CCEW and MJO phenomenon during the Asia-Australian monsoon phase over Indonesia. The filtered waves from 15-year of TRMM 3B42 data are compared with rainfall anomaly among 38-synoptic stations during both active and extreme monsoon phases. The results show that CCEW is predominant during DJF-WNP over Indonesia while moving away toward northern off-equatorial during JAS-AU, particularly for MRG and IG1 (cf. Wheeler and McBride 2005; Kiladis et al. 2009; Horinouchi 2012; Lubis and Jacobi 2014). Meanwhile, MJO has been proven to triggers convection over Indonesia (Madden and Julian 1972; Hidayat and Kizu 2010), even though seems to be more predominant during DJF-WNP, while moving toward northern hemisphere away from Indonesia during JAS-AU. By classifying the WNP and AU monsoon phases into all active and extreme monsoon phases based on their climatology thresholds, a distinction between each wave was observed, where the MJO controlled a deep convection stronger during all active monsoon phases than during extreme phases. On the other hand, the extreme monsoon phase controls deep convective clouds associated with Kelvin, ER, MRG, and IG1 stronger compared with an active monsoon phase, particularly during DJF-WNP for IG1.

Even though not too vigorous, there is still an influence of wave activity against rainfall variability related to the WNP and AU monsoons over Indonesia. As the most predominant wave that controls rainfall variability over Indonesia, the MJO is adequate to control rainfall anomaly during all active monsoon phases for all wave perturbation values, approximately 62.37% stronger than the undefined wave–rainfall anomaly relationship. The Kelvin wave has given a significant impact in determining rainfall activity during the monsoon phase for more than 60%, which mainly increases rainfall anomaly during DJF-WNP over western Indonesia (cf. Wheeler and McBride 2005). Meanwhile, an unorganized positive wave–rainfall anomaly relationship distribution is exhibited for an off-equatorial ER wave, even though still evoking a remaining wave-impacted area over northern boundaries of Indonesia, i.e., northern Sulawesi. On the other hand, the influenced area by MRG wave during DJF-WNP is rather being ignored by its climatological predominant area (Kiladis et al. 2009). However, a distinction that emerged from this study is that there is still a high positive relationship (78.75%) especially during the JAS-AU extreme monsoon phase for the significant MRG value, which is consistent with findings from Horinouchi (2012). This result may suggest that a positive (negative) significant MRG perturbation area, indicated by dark (light) dashed shadow area in Fig. 11, generates a positive (negative) rainfall anomaly in the southern hemisphere of Indonesia. Meanwhile, IG1 has given a dominant impact over the eastern part of Indonesia, even though a further study has

to be made due to the lack of observational data station in this area (especially Maluku and Papua).

Notwithstanding, extreme monsoon phase did not robustly contribute to influence rainfall anomaly associated with CCEW and MJO; this monsoon classification has proven to control rainfall activity related to CCEW and MJO during DJF-WNP (60.66%) for only a significant wave perturbation value. However, a positive wave–rainfall anomaly relationship seems to be more prominent during DJF-WNP than during the JAS-AU monsoon phase, although there is still a wave that indicates a prominent relationship during JAS-AU (i.e., MRG). Meanwhile, CCEW and MJO significantly increase/decrease precipitation at Day 0 for about 37.88% from total Day 1st to Day end. Although the contribution of CCEW and MJO were not too abundant to influence rainfall activity during monsoon phase over Indonesia, these two events still modulate weather conditions for more than 50% (cf. Wheeler and McBride 2005; Kiladis et al. 2009; Hidayat and Kizu 2010; Horinouchi 2012; Lubis and Jacobi 2014). The negative impacts of these waves, particularly MJO, are generally due to a dominant local factor from a complex topography that lies over the region of Indonesia, which also agree with previous studies by Hidayat and Kizu (2010) and Huang and Huang (2011).

Eventually, as a consequence of two big oceans (the Indian Ocean and the Pacific Ocean) that lie between Indonesia, the interaction between ocean and atmosphere (e.g., IOD and ENSO) should be a consideration for further study (cf. Sein and Zhi 2016). Moreover, a further study with a more complex data particularly over the eastern part of Indonesia is required to obtain a more detailed analysis of the local complexities which are influenced by the CCEW including the MJO.

**Acknowledgements** The authors are also very grateful to Mr. George Kiladis (NOAA) for allowing the adaptation of WK99 method in this study. The authors also want to thank Mrs. Juliana Dias (NOAA) and Mr. Zhong Liu (NASA) for their great assistance.

**Funding information** This research is supported by the National Aeronautics and Space Administration (NASA)-Goddard Earth Sciences Data and Information Services Center (GES DISC) for TRMM 3B42 V7 dataset and by the European Centre for Medium-Range Weather Forecasts (ECMWF) for ERA-Interim reanalysis dataset. The authors would like to thank the Head of the Indonesian Meteorological Climatological and Geophysical Agency (BMKG) for the full scholarship in Gadjah Mada University (UGM), Faculty of Geography, as well as the Head of the Education and Training Center (Pusdiklat BMKG).

## References

- Aldrian E, Susanto D (2003) Identification of three dominant rainfall regions within Indonesia and their relationship to sea surface temperature. *Int J Climatol* 23:1435–1452
- Cho HK, Bowman KP, North GR (2004) Equatorial waves including the Madden Julian Oscillation in TRMM rainfall and OLR data. *J Clim* 17:4387–4406

- Dee DP (2011) The ERA-interim reanalysis: configuration and performance of the data assimilation system. *Q J R Meteorol Soc* 137: 553–597
- Gill AE (1982) Studies of moisture effects in simple atmospheric models: the stable case. *Geophys Astrophys Fluid Dyn* 19:434–438
- Hidayat R, Kizu S (2010) Influence of the Madden–Julian Oscillation on Indonesian rainfall variability in austral summer. *Int J Climatol* 30: 1816–1825
- Holton JR (2004) An introduction to dynamic meteorology. In: , International geophysical series, vol 88, 4th edn. Academic Press, pp 553, 394–403
- Horinouchi T (2012) Modulation of seasonal precipitation over the tropical Western/Central Pacific by convectively coupled mixed Rossby–gravity waves. *J Atmos Sci* 70:600–606
- Huang A, Huang R (2011) Climatology and interannual variability of convectively coupled equatorial waves activity. *J Clim* 24(12): 4451–4465
- Huffman GJ (2006) The TRMM multisatellite precipitation analysis (TMPA): quasi-global, multiyear, combined-sensor precipitation estimates at fine scales. *J Hydrometeorol* 8:38–55
- Kikuchi K, Kiladis GN, Dias J, Nasuno T (2018) Convectively coupled equatorial waves within the MJO during CINDY/DYNAMO: slow Kelvin waves as building blocks. *Clim Dyn* 50:4211–4230
- Kiladis G, Wheeler M, Haertel P, Straub K, Roundy P (2009) Convectively coupled equatorial waves. *Rev Geophys* 47:RG2003
- Koseki S, Koh TY, Teo CK (2014) Borneo vortex and mesoscale convective rainfall. *Atmos Chem Phys* 14:4539–4562
- Liebmann B, Hendon HH (1990) Synoptic-scale disturbances near the equator. *J Atmos Sci* 47:1463–1479
- Lodangco C, Leslie LM (2016) Cluster analysis of Philippine tropical cyclone climatology: applications to forecasting. *J Climatol Weather Forecasting* 4:1–17
- Lubis SW, Jacobi C (2014) The modulating influence of convectively coupled equatorial waves (CCEWs) on the variability of tropical precipitation. *Int J Climatol* 35:1465–1483
- Madden RA, Julian PR (1972) Description of global-scale circulation cells in the tropical with 40–50 day period. *J Atmos Sci* 29:1109–1123
- Matsuno T (1966) Quasi-geostrophic motions in the equatorial area. *J Meteor Soc Japan* 44:25–43
- NASDA (2001) TRMM data users handbook. NASDA 226
- Ramage CS (1971) Monsoon meteorology. International geophysical series, vol. 15, Academic Press, 296 pp, 139–141 and 186–188
- Sein ZMM, Zhi X (2016) Interannual variability of summer monsoon rainfall over Myanmar. *Arab J Geosci* 9:469
- Takayabu YN, Nitta T (1993) 3–5 day period disturbances coupled with convection over the tropical Pacific Ocean. *J Meteor Soc Japan* 71: 221–246
- Wang B, Fan Z (1999) Choice of south Asian summer monsoon indices. *B. American Meteor. Soc.* 80:629–638
- Wang B, Liu J, Kim HJ, Webster PJ, Yim SY (2012) Recent change of the global monsoon precipitation (1979–2008). *Clim Dyn* 39:1123–1135
- Wheeler MC, Kiladis GN (1999) Convectively coupled equatorial waves: analysis of clouds and temperature in the wavenumber-frequency domain. *J Atmos Sci* 56:374–399
- Wheeler MC, McBride JL (2005) Australian-Indonesian monsoon. In: Lau WKM, Waliser DE (eds) Intraseasonal variability in the atmosphere-ocean climate system. Springer, Heidelberg, pp 125–173
- Yanai M, Maruyama T (1966) Stratospheric wave disturbances propagating over the equatorial Pacific. *J Meteor Soc Japan* 44:291–294
- Yanai M, Maruyama T, Nitta T, Hayashi Y (1968) Power spectra of large-scale disturbances over the tropical Pacific. *J Meteor Soc Japan* 46: 308–323
- Yim SY, Wang B, Liu J, Wu Z (2013) A comparison of regional monsoon variability using monsoon indices. *Clim Dyn* 43:1423–1437
- Zhao C, Li T, Zhou T (2013) Precursor signals and processes associated with MJO initiation over the tropical Indian Ocean. *J Climate* 26: 291–307